MCP Papers in Press. Published on June 2, 2017 as Manuscript M116.066381

ASBMB MOLECULAR & CELLULAR PROTEOMICS MCP

# Proteome-wide identification of glycosylation-dependent interactors of Galectin-1 and Galectin-3 on mesenchymal retinal pigment epithelial cells

Jara Obermann[1], Claudia S. Priglinger[2], Juliane Merl-Pham[1], Arie Geerlof[3], Sigfried Priglinger[2], Magdalena Götz[4,5], Stefanie M. Hauck[1]

1. Research Unit Protein Science, Helmholtz Center Munich, German Research Center for Environmental Health (GmbH), Neuherberg, Germany
2. Department of Ophthalmology, Ludwig-Maximilians-University, Munich, Germany
3. Protein Expression and Purification Facility, Institute of Structural Biology, Helmholtz Center Munich, German Research Center for Environmental Health (GmbH), Neuherberg, Germany
4. Institute of Stem Cell Research, Helmholtz Center Munich, German Research Center for Environmental Health (GmbH), Neuherberg, Germany
5. Physiological Genomics, Biomedical Center, Ludwig-Maximilians-University, Munich, Germany

To whom correspondence about the manuscript should be addressed:

Stefanie Hauck, Research Unit Protein Science, Helmholtz Center Munich, German Research Center for Environmental Health (GmbH), Heidemannstr.1, 80939 München, Germany, Ph.: +49-89-3187-3941, e-Mail: hauck@helmholtz-muenchen.de

**Running Title: Galectin-1 and Galectin-3 interactors**



Copyright 2017 by The American Society for Biochemistry and Molecular Biology, Inc.

ASBMB MOLECULAR & CELLULAR PROTEOMICS MCP

## Abbreviations page

α2M: alpha-2-macroglobulin

ABC: ammonium bicarbonate

CD: cluster of differentiation

CNBr: cyanogen bromide

CRD: carbohydrate recognition domain

DAPI: 4',6-diamidino-2-phenylindole

DMEM: Dulbecco's modified Eagles medium

ECM: extracellular matrix

EGF: epidermal growth factor

EMT: epithelial-to-mesenchymal transition

FC: fold change

FDR: False Discovery Rate

Gal-1: Galectin-1

Gal-3: Galectin-3

GAPDH: Glyceraldehyde 3-phosphate dehydrogenase

GFP: green fluorescent protein

GO: gene ontology

ASBMB MOLECULAR & CELLULAR PROTEOMICS MCP

HRP: horseradish peroxidase

ITGB1: integrin beta 1

LAMP: lysosomal-membrane-associated glycoprotein

LRP1: low-density lipoprotein receptor

MAPK: mitogen-activated protein kinase

NCAM: neural cell adhesion molecule

PDGFRB: platelet-derived growth factor receptor beta

PVR: proliferative vitreoretinopathy

RBC: red blood cell

RMG: retinal Müller glial cells

RPE: retinal pigment epithelial cells

RT: room temperature

TGF-β: transforming growth factor beta

TXR: texas red

UA: urea

VEGF: vascular endothelial growth factor

ASBMB MOLECULAR & CELLULAR PROTEOMICS MCP

**Summary**

Identification of interactors is a major goal in cell biology. Not only protein-protein but also protein-carbohydrate interactions are of high relevance for signal transduction in biological systems. Here we aim to identify novel interacting binding partners for the β-galactoside-binding proteins Galectin-1 (Gal-1) and Galectin-3 (Gal-3) relevant in the context of the eye disease proliferative vitreoretinopathy (PVR). PVR is one of the most common failures after retinal detachment surgeries and is characterized by the migration, adhesion and epithelial-to-mesenchymal transition (EMT) of retinal pigment epithelial cells (RPE) and the subsequent formation of sub- and epiretinal fibrocellular membranes. Gal-1 and Gal-3 bind in a dose- and carbohydrate-dependent manner to mesenchymal RPE cells and inhibit cellular processes like attachment and spreading. Yet knowledge about glycan-dependent interactors of Gal-1 and Gal-3 on RPE cells is very limited, although this is a prerequisite for unravelling the influence of galectins on distinct cellular processes in RPE cells. We identify here 131 Gal-3 and 15 Gal-1 interactors by galectin pull-down experiments combined with quantitative proteomics. They mainly play a role in multiple binding processes and are mostly membrane proteins. We focused on two novel identified interactors of Gal-1 and Gal-3 in the context of PVR: the low-density lipoprotein receptor LRP1 and the platelet-derived growth factor receptor beta PDGFRB. Addition of exogenous Gal-1 and Gal-3 induced crosslinking with LRP1/PDGFRB and Integrin-β1 (ITGB1) on the cell surface of human RPE cells and induced ERK/MAPK and Akt signaling. Treatment with Kifunensine, an inhibitor of complex-type-N-glycosylation, weakened the binding of Gal-1 and Gal-3 to these interactors and prevented lattice formation. In conclusion, the identified specific glycoprotein ligands shed light into the highly specific binding of galectins to dedifferentiated RPE cells and the resulting prevention of PVR-associated cellular events.

ASBMB MOLECULAR & CELLULAR PROTEOMICS MCP

## Introduction

Galectins are widely expressed across different species and organs and share homology in the amino acid sequence of their carbohydrate recognition domain (CRD)[1-4]. They interact with their protein ligands by binding to β-galactoside containing moieties on the glycosylated peptide backbones[1, 5, 6]. Thereby they decipher the information stored in the glycan chains and can substantially influence many cellular functions including attachment, spreading, migration and proliferation[7, 8]. Galectins can be subdivided into three classes based on their molecular structure: proto-, chimera and tandem-repeat type[3]. Galectin-3 (Gal-3) is the only known chimera type galectin of the human lectin family[1, 9, 10]. It consists of a C-terminal domain to bind specific carbohydrate branches and an N-terminal domain, which enables Gal-3 to multimerize[1, 11]. Via the C-terminal domain, Gal-3 can cross-link glycoproteins on the plasma membrane and thus induce cell surface lattice formation[11]. Galectin-1 (Gal-1) is assigned to the prototype galectins, consisting of one CRD[9]. By hydrophobic interactions at the N-terminal amino acid residues, prototype galectins can self-associate their monomer subunits to form homodimers[4, 12, 13]. These dimers can crosslink specific multivalent carbohydrates or glycoconjugates, which results in the formation of cross-linked lattices and the activation of several cellular pathways [4, 14-17].

Proliferative vitreoretinopathy (PVR) is a blinding disease frequently occurring as a complication after rhegmatogenous retinal detachment surgery[18-21]. It is characterized by the formation of sub- and epiretinal fibrocellular membranes, which contract and lead to repetitive tractional retinal detachment [20, 22-24]. Adhesion, migration and epithelial-to-mesenchymal transition (EMT) of retinal pigment epithelial cells (RPE) and retinal Müller Glial cells (RMG) are the key cellular events in the onset of PVR[20, 23, 25]. During EMT RPE cells convert from epithelial into mesenchymal cells and lose their epithelial characteristics and acquire migratory mesenchymal

properties[26]. Cultured human RPE cells are a well-accepted in vitro model system for early PVR. By cultivating RPE cells on plastic, they begin to dedifferentiate and to transform into a fibroblast-like phenotype[27]. Gal-1 and Gal-3 are endogenously expressed in RPE cells. They are present in the cytosol and nucleus, but they are also secreted by a non-classical pathway to the cell surface[28]. Extracellularly, Gal-1 and Gal-3 are involved in cell-matrix and cell-cell interactions[8]. As shown in previous studies, exogenous Gal-1 and Gal-3 bind carbohydrate-dependent to mesenchymal RPE and inhibit attachment and spreading of these cells [29, 30]. We also demonstrated that EMT of RPE cells leads to increased β-1,6-N-glycosylation on the cell surface resulting in increased binding capacity of Gal-3[31]. Most of the recent experimental therapeutic approaches attempted to control PVR development by anti-proliferative or anti-inflammatory agents or by inhibition of single growth factors and their signaling pathways[32-39]. However, PVR is a multifactorial, mostly cell driven process, which requires a multimodal concept[24]. Identification of a pharmacological agent that is capable to govern several cellular processes simultaneously is necessary to treat PVR. Thereby, Gal-1 and Gal-3 bear a high potential to counteract PVR-associated cellular events.

However, while the cell surface proteins on RPE cells targeted by specific galectins are largely unknown, this in-depth knowledge is a prerequisite to unravel the possible influence of galectins on the signal transduction mechanisms associated with PVR processes. In many other cell types several interactors for Gal-1 or Gal-3 have been identified: these include among others lysosomal-membrane-associated glycoproteins (LAMPs)-1 and -2, neural cell adhesion molecule (NCAM), cell adhesion molecule L1, CD43, CD45, CD71, mucin-1 and receptors for distinct growth factors like the epidermal growth factor (EGF), transforming growth factor beta (TGF-β) or vascular endothelial growth factor (VEGF)[5, 40-50]. Extracellular matrix (ECM) proteins like laminin, fibronectin or vitronectin as well as members of the β1 integrin family are also known Gal-1 and Gal-3 interactors[5, 46, 49, 51-53]. Integrins play a major role in cell-matrix-



ASBMB MOLECULAR & CELLULAR PROTEOMICS MCP

ASBMB MOLECULAR & CELLULAR PROTEOMICS MCP

interactions. As transmembrane proteins they are able to bind to the ECM by their extracellular part and induce several signal transduction cascades in the cell, e.g. remodeling of the cytoskeleton or proliferation[51, 54]. Priglinger et al. [42] showed that Gal-3 induces clustering of CD147 and integrin-β1 (ITGB1) transmembrane glycoprotein receptors on the RPE cell surface. However, the functional relevance of galectin-binding on these different receptors is not explicitly analyzed in context of PVR.

The purpose of this study was to identify novel specific glycoprotein ligands for Gal-1 and Gal-3 on the surface of mesenchymal RPE cells by an affinity capture quantitative LC-MSMS based approach. From the 131 and 15 specific interactors identified for Gal-3 and Gal-1, respectively, we focused on two novel interactors for functional validation of the PVR relevant cellular behavior: the low density lipoprotein receptor-related protein (LRP1) and the platelet-derived growth factor receptor beta (PDGFRB). Addition of Gal-1 and Gal-3 induced clustering with the identified glycoprotein receptors LRP1 and PDGFRB together with ITGB1 on RPE cell surfaces, validating their potential to influence cellular effects. Relevance of glycosylation of these interactors for the functional galectin binding and the crosslinking activity was also analyzed.

ASBMB MOLECULAR & CELLULAR PROTEOMICS MCP

## Experimental Procedures

### Isolation of Human RPE Cells and Human RPE Cell Culture

Human cadaver eyes of donors were received by the Eye Bank of the Department of Ophthalmology at the Linz General Hospital (Linz, Austria) or at the Ludwig-Maximilians-University (LMU) (Munich, Germany) and were processed within 24 hours after death as described in Priglinger et al. [42] and Priglinger et al. [31]. The securing processes of the human tissue were humane, complied with the Declaration of Helsinki and were approved by the relatives. The ethics committees of the hospital of the LMU Munich and of the Land Oberoesterreich authorized the procedure of isolation of RPE cells from human cadaver eyes, which were enucleated by an ophthalmologist in accordance with the institutions standard operating procedures. After removal of the cornea for cornea-transplantation, the front segment of the eye and the vitreous body were removed. The inner part of the rest of the eye was filled with phosphate-buffered saline (PBS, Gibco) and the retina was aspirated. To get rid of the remaining retina and photoreceptors, the eye was refilled with pre-warmed 1mM EDTA in PBS (37°C), pH 7.4, and incubated for 15-20 min at room temperature. PBS/1mM EDTA was aspirated and the eyecup was filled with dissociation buffer (3 mM L-Cystein, 1µg/µl BSA in PBS/1mM EDTA), containing 45µg papain (Worthington) per 1ml dissociation buffer. After incubation for 23 minutes at 37°C, the solution within the eye was gently agitated with a pipette to dispense as much RPE cells as possible. The loosened RPE cells were transferred in Dulbecco's modified Eagles medium (DMEM; Gibco) supplemented with 10% fetal calf serum (FCS; Gibco) and centrifuged for 5 minutes at 930 rpm at room temperature. The resuspended RPE cells were cultivated in DMEM, 10% FCS at 37°C and 5% $CO_2$ with or without 10µM Kifunensine for up to 4 weeks (Sigma Aldrich). Primary human RPE cells of passage 4 to 7 were used for experiments. For some experiments the human ARPE-19 cell line (ATCC® CRL-

2302™) was used[55]. ARPE-19 cells were cultivated under the same cell culture conditions like primary RPE cells. For preparation of protein lysates, RPE cells were washed with ice-cold PBS, collected and lysed in RIPA buffer (50 mM Tris-HCl pH 7.4, 150 mM NaCl, 0.1%(w/v) SDS, 0.5% (w/v) Sodium Deoxycholate, 1% (v/v) NP-40, Complete 1X).

**Expression, purification, biotinylation and activity control of human galectin-1 and -3**

Human Gal-1 and Gal-3 were cloned in the bacterial pETM-11 expression vector as previously described[31, 42]. The single modification was that his6-tagged hGalectin-1 was dialyzed against PBS containing 5 mM β-mercaptoethanol at the end of the purification process. For biotinylation, 150mM ß-Lactose was added to 1 mg of purified Gal-1 and Gal-3 and the proteins were dialyzed for 2 hours at 4°C against 0.1M sodiumhydrogencarbonate with 50 mM ß-Lactose, pH 9.2., followed by a 1 hour biotinylation at RT with 100µg biotinamidohexanoic acid N-hydroxysuccinimide ester according to the manufacturer´s instructions (Sigma Aldrich). The biotinylated galectins were dialyzed overnight at 4°C against PBS. Activity of biotinylated galectins was determined semi-quantitatively by hemagglutination assays, adapted from Nowak et al. [56] and St-Pierre et al. [57]. Briefly, for preparation of type 0 red blood cells (RBC), 6 ml whole blood samples were collected in EDTA tubes and centrifuged at 3500 rpm for 5 min. After removal of the transparent layer, RBCs were washed 3 times in PBS, diluted 1:10 in PBS-3% glutaraldehyde and rotated for 1h at room temperature. RBCs were washed 5 times in PBS-0.0025% $NaN_3$ and resuspended at 4% in PBS-0.0025 $NaN_3$ to preserve it for 3 months. For hemagglutination assay, serial dilutions of galectins were put in U-shaped 96 well plates and 10µl RBCs were added per well. After incubation at 37°C for 30 min, the minimum active concentration of each galectin, that prevented sedimentation of the RBCs, was evaluated visually. For further experiments Gal-1 and Gal-3 were used in sufficiently active concentrations, as specified respectively.



ASBMB MOLECULAR & CELLULAR PROTEOMICS MCP

ASBMB MOLECULAR & CELLULAR PROTEOMICS MCP

**Galectin pull-down experiments**

For galectin pull down experiments, 1mg Gal-1 or 1mg Gal-3 were coupled on 300mg cyanogen bromide-activated Sepharose 4B (GE Healthcare). First the Sepharose beads were activated by washing 15 times with 1mM HCl, followed by a single washing step in coupling buffer (0.1M NaHCO3, 0.5M NaCl, pH 8.3). All washing steps included a centrifugation at 3000 rpm for 1 minute. Galectins were mixed 1:1 with coupling solution and were incubated on a rotating wheel with the activated beads at 4°C overnight. After washing with a 5 fold volume of coupling buffer, unreacted binding sites were blocked with 1M ethanolamine (pH8) for 2 hours at room temperature. Several subsequent washing steps followed at different pH values (3x coupling solution, 3x acetate buffer (0.1M NaAc, 0.5M NaCl, pH 3-4), 3x coupling buffer, 3x acetate buffer, 3x PBS). The galectin-beads were stable for several months, when stored in 20% ethanol. To test, whether the respective galectin, coupled to the beads, was still active, 100µl beads-slurry (50% beads) was incubated with 200µg asialofetuin (Sigma) for 1h at RT in absence and presence of 0.1M ß- lactose. After washing with PBS, bound proteins were eluted by incubation with 3x Laemmli buffer at 95°C for 5 min. Eluates were separated by SDS-PAGE (10% gels) and asialofetuin was detected by Coomassie staining (supplemental figure 1). For galectin pull-downs 250µg total proteins from human mesenchymal RPE cell lysates were incubated with 20µl galectin-beads-slurry or ProteinG control beads-slurry (GE Healthcare) in PBS for 1h at 37°C, with gentle mixing every 10 min. After centrifugation, beads were washed 4 times with PBS followed by elution of bound proteins with 0.5M β-lactose (sigma). Eluates were analysed by label-free quantitative LC-MS/MS. Five independent Gal-3 and five independent Gal-1 as well as the corresponding control ProteinG pull-down experiments with 3 or 4 technical replicates each were performed using RPE cell lysates derived from nine different human donors.

ASBMB MOLECULAR & CELLULAR PROTEOMICS MCP

**Sample preparation for mass spectrometry**

ß-lactose eluates of the Gal-1, Gal-3 and ProteinG pull-down experiments were proteolysed with Lys-C and trypsin (Promega, Mannheim, Germany) using a modified filter aided sample preparation protocol [58]. Briefly, protein eluates were diluted with ammonium bicarbonate buffer (ABC, Sigma) to a final volume of 100µl, followed by reduction using 1µl 1M dithiothreitol (DTT) for 30 min at 60°C. After cooling down to RT, 100µl 8M Urea Buffer (UA, Sigma), pH 8.5, was added and proteins were alkylated with 10µl 300 mM iodoacetamide (Merck) for 30 min at RT in the dark. 2µl 1M DTT was added to quench unreacted iodacetamide and protein eluates were transferred to 30 kDa cut-off centrifuge filter (Pall Corporation, NY). After washing 3 times with 400µl UA buffer and twice with 100µl 50mM ABC, the proteins were subjected to a 2h digest at RT with 1µg Lys-C followed by tryptic digest (2µg trypsin) overnight at 37°C. Peptides were collected by centrifugation through the filter and acidified with trifluoroacetic acid (TFA) (pH2).

**Mass Spectrometry**

LC-MS/MS analysis was performed as described previously on a LTQ OrbitrapXL (Thermo Fisher Scientific Inc.) [59-62]. Briefly, every sample was automatically loaded onto an Ultimate3000 nano HPLC system (Dionex) with a nano trap column (300 µm inner diameter × 5 mm, packed with Acclaim PepMap100 C18, 5 µm, 100 Å; LC Packings, Sunnyvale, CA) at a flow rate of 30µl/min in HPLC buffer containing 0.1% trifluoroacetic acid (TFA) for 5 minutes. Peptides were separated on a reversed phase chromatography (PepMap, 25 cm, 75µm ID, 1µm/100 Å pore size, LC Packings) over 80 or 140 minutes at a flow rate of 300 nl/min using increasing ACN concentrations in 0.1% formic acid. Maximal injection time for MS spectra was 100ms, for MSMS spectra 500ms. MS data were acquired using from the high resolution MS prescan the 10 most abundant peptide ions for fragmentation in the linear ion trap, if they were at least doubly charged and have an intensity of at least 200 counts, with a dynamic exclusion of 45

ASBMB MOLECULAR & CELLULAR PROTEOMICS MCP

seconds and an isolation width of 2 amu. MS spectra were recorded within a mass range from 300 to 1500 m/z at a resolution of 60,000 full widths at half-maximum. The mass spectrometry data have been deposited to the ProteomeXchange Consortium via the PRIDE[63] partner repository with the dataset identifier PXD005461 and 10.6019/PXD005461.

**Protein Identification and label-free Quantification**

The acquired spectra of the different samples were analyzed using Progenesis QI software for proteomics (Version 2.0, Nonlinear Dynamics, Waters, Newcastle upon Tyne, U.K.) for precursor intensity-based label-free quantification, as previously described [59-62]. Peak lists with respective m/z values, intensities, abundances and m/z width were generated out of the profile data of the MS scans. MS/MS spectra were also transformed and stored in peak lists incorporating m/z and abundance. The retention times of all samples were aligned to the most complex sample as reference. Alignment to a maximal overlay of all 2D features was done both automatically and manually. Only features with charges of at least 2 and not more than seven were included in further analyses. After alignment and feature exclusion, samples were divided into their respective experimental groups (Gal1, Gal3, ProtG lactose eluates), and raw abundances of all features were normalized. Peptide identification was done with Mascot (MatrixScience, London, UK; version 2.5.1) using the Ensembl human protein database (homo sapiens, release: 75, 105287 sequences; release: 80, 100208 sequences). The parameters for the search were cleavage with trypsin, 0.6 Da fragment mass tolerance and 10 ppm peptide mass tolerance. Carbamidomethylation was set as fixed modification, and methionine oxidation and deamidation of asparagine and glutamine as variable modifications. One missed cleavage was allowed. A Mascot-integrated decoy database search calculated an average false discovery (FDR) of <1.25% when searches were performed with a mascot percolator score cut-off of 15 and an appropriate significance threshold p. Peptide assignments were reimported into

ASBMB MOLECULAR & CELLULAR PROTEOMICS MCP

Progenesis QI and all normalized abundances of unique peptides of an identified protein were summed to calculate the total cumulative normalized abundance of the respective protein. These abundances were used to calculate the enrichment factors of the quantified proteins in the lactose eluates of the galectin pull-downs compared to ProteinG pull-downs. No minimal thresholds were set neither for the method of peak picking nor selection of data to use for quantification.

**Experimental Design and Statistical Rationale**

Five independent Galectin-1 and Galectin-3 as well as the corresponding control ProteinG pull-down experiments with nine different biological samples were performed, each including 3 or 4 technical replicates. Statistical analysis was done using normalized abundances of all identified proteins using only unique peptides. For calculation of the enrichment factors of proteins in the lactose eluates of galectin pull-downs compared to unspecific controls, the mean of all technical replicates within one experiment was used. Normal distribution was assumed and significance was determined by Student's t-test. Proteins with p-values $<0.05$, enrichment of $\geq$ two-fold in galectin pull-down eluates (FC $\geq$ 2) which were identified in two or more independent experiments were regarded as potential Gal-1 or Gal-3 interactors.

**Volcano Plots, Cellular Component and Network Analysis**

Volcano plot representations of Gal-1 and Gal-3 pull-down experiments were done with Excel. The x-axis shows the log2 transformed ratio between normalized abundances of proteins identified in lactose eluates of galectin pull-down compared to unspecific control (ProtG pull-down). The y-axis gives the negative log10 transformed p-value from the t-test of the same two comparisons. P-values $<0.05$ and FC $\geq$ 2 were regarded as significant. Infinite fold changes were set to the highest measured ratio plus 1, fold changes with a value of 0 were equalized

ASBMB MOLECULAR & CELLULAR PROTEOMICS MCP

with the lowest measured ratio. Cellular component analysis of the 15 identified Gal-1 interactors and the 131 Gal-3 interactors was performed based on the gene ontology (GO) annotation "cellular component" in FunRich[64]. For protein network generation, the corresponding gene names of the Gal-1 and Gal-3 interactors were uploaded in the Cytsocape App ClueGO-CluePedia[65] and clustered by the GO term "molecular function" using homo sapiens as the organism for background list. The size of the nodes represents the enrichment significance of the respective terms based on the predefined kappa score threshold of 0.4. The ClueGO network reflects the relationship between the respective functional groups represented by their most significant (leading) term. With the identified Gal-1 and Gal-3 interactors, Phobius analysis was done to predict based on the amino acid sequence of a protein, if the respective protein has a transmembrane domain and signal peptides[66].

**Immunocytochemical staining**

Mesenchymal human RPE cells were cultivated on glass coverslips (VWR) upon 60-70% confluence in DMEM+10% FCS with or without 10µM Kifunensine (Sigma Aldrich) up to passage 4-7. Before fixation with 4% paraformaldehyde, cells were starved for 2 hours in serum-free DMEM and treated with biotinylated Gal-1 and Gal-3 with a final concentration of 120µg/ml Gal-1 or 60µg/ml Gal-3 for 30 minutes at 37°C. As control no galectin was added. After blocking (Tris-buffered saline with 0.1% Tween20 (TBS-T)+1%bovine serum albumin (BSA)+0.5% goat serum) for 45 minutes at RT, galectin binding was visualized by incubation with Streptavidin-Alexa488 (1:500, ThermoFisher) for 1h at RT. Coverslips were incubated overnight at 4°C in rabbit anti-LRP1 (1:50, abcam), rabbit anti-PDGFRB (1:50, abcam) or rat anti-ITGB1 (1:60, DSHB) diluted in TBS-T, followed by incubation with goat-anti-rabbit-AlexaFluor647 or goat anti-rat AlexaFluor568 (1:1000, Dianova) for 1h at RT. Between each staining step at least one washing step was executed with TBS-T for 10 min. After

ASBMB MOLECULAR & CELLULAR PROTEOMICS MCP

counterstaining with Hoechst (1:5000, ThermoFisher) for 8 minutes at RT, coverslips were mounted and photographed on a Leica DMi8 microscope with a HCX PL APO 63x/1.20 objective lens. Filter cubes for GFP, Y5, TXR and DAPI detections were used (JH Technologies). All images were captured using a Leica DFC365 FX camera and constant settings for gain and exposure time were maintained for all samples within an experimental set-up. Images were processed by the Leica Application Suite LASX (version 2.0, Leica) and the deconvolution software Huygens Essential using the classic maximum likelihood estimation (CMLE) algorithm with a signal to noise ratio of 40 and 50 iterations (version 16.05, Scientific Volume Imaging B.V., Netherlands, http://svi.nl). As control, cells were stained under equal conditions without primary antibodies and only with secondary antibodies. No unspecific labeling was observed (data not shown). Immunocytochemical staining of human RPE cells was repeated at least three times with cells from three different donors.

**Western Blot analysis**

Eluates of the Gal-1 and Gal-3 pull-down experiments with lysates of mesenchymal RPE cells from three different donors, treated or untreated with 10µM Kifunensine for up to 4 weeks, were separated by SDS-PAGE (10% gels) and blotted onto PVDF membranes. Ten microgram of the whole cell extracts of the respective cell lysates were used as an input control for the pull-down experiments. After blocking with 5% non-fat dried milk in TBS-T for 1h at RT, blots were incubated with antibodies against rabbit anti-LRP1 (1:20,000, abcam), rabbit anti-PDGFRB (1:1,000, abcam) or mouse anti-GAPDH (1:10,000, Millipore) at 4°C overnight. For analysis of phosphorylation changes of ERK after galectin treatment, 15µg of whole cell extracts of ARPE19 cells untreated or treated with 120µg/ml Gal-1 or 60µg/ml Gal-3 for 1, 15 or 30 minutes were separated by SDS-PAGE (10% gels) and blotted onto PVDF membranes. Blocking was performed with 3% BSA in TBS-T for 1 hour and blots were incubated with antibodies against

rabbit anti-phospho-ERK p44/p42 (1:2,000, cell signaling, #4370) and mouse anti-GAPDH (1:10,000, Millipore) at 4°C overnight. After washing three times with TBS-T, blots were incubated with the appropriate HRP-coupled secondary antibodies (1:7,500, Jackson ImmunoResearch) for 1h at RT and binding was visualized by signal development with ECL Plus enhanced chemiluminescence kit (GE Healthcare). Galectin pull-down experiments with following Western Blot analysis were repeated at least 3 times on three different RPE lysates.

**Analysis of phosphorylation profiles**

For the simultaneous analysis of relative changes in site-specific phosphorylation profiles of 43 kinases and 2 related total proteins after galectin treatment, the Human Phospho-Kinase Array (R&D Systems, ARY003B) was used. Selected phospho-specific capture antibodies were spotted in duplicate on nitrocellulose membranes. According to the manufacturer´s instructions (R&D systems), 300µg of whole cell extracts of ARPE19 cells untreated or treated for 15 minutes with 120µg/ml Gal-1 or 60µg/ml Gal-3 were incubated with the nitrocellulose membranes overnight at 4°C. After subsequent incubation with a cocktail of biotinylated detection antibodies and Streptavidin-Horseradish Peroxidase, the amount of phosphorylated protein bound at the respective capture spot was visualized by signal development with chemiluminescent detection reagents. Pixel density of each spot was determined with ImageJ considering background subtraction[67]. Mean pixel density, standard deviation and statistical significance (Student's t-test) were determined. P-values lower than 0.05 were considered as significant (*), p-values lower than 0.01 as highly significant (**).



ASBMB MOLECULAR & CELLULAR PROTEOMICS MCP

ASBMB MOLECULAR & CELLULAR PROTEOMICS MCP

## Results

### Galectin-3 revealed more interacting binding partners than galectin-1

To identify Gal-1 and Gal-3 specific binding proteins in dedifferentiated mesenchymal human RPE cells, the respective galectin was coupled to CNBr-activated sepharose beads and incubated with RPE cell lysates. Interacting proteins were eluted by β-lactose as competitor for specific carbohydrate binding. To exclude unspecific binders, the same pull-down experiments were performed with ProteinG-coupled sepharose beads. A subsequent proteomic screening of these lactose eluates revealed identification of 1429 different proteins in all 5 independent Gal-3 pull-down experiments (with 3 or 4 technical replicates each, supplemental data S1 and S2) and 1528 different proteins in 5 independent Gal-1 pull-down experiments (3 or 4 technical replicates per experiment, supplemental data S3 and S4) (figure 1A, left) with an overlay of 1272 proteins. To identify the most promising Gal-1 and Gal-3 interactors, those proteins, that were significantly ($p<0.05$) at least 2-fold (fold-change (FC)≥2) enriched in Gal-1 or Gal-3 eluates compared to the unspecific control, were selected. 771 proteins in Gal-3 pull-down experiments were specifically enriched in the Gal-3 lactose eluates (FC≥2) and 332 of these proteins reached significance (FC≥2, $p<0.05$) (figure 1A, middle). In contrast to that, while 698 proteins were over 2-fold enriched in Gal-1 eluates (FC≥2), only 60 proteins could be determined as significantly bound to Gal-1 (FC≥2, $p<0.05$) (figure 1A, middle). Consequently, Gal-3 revealed more significant interacting binding partners than Gal-1, which is represented in the volcano plots of one exemplary Gal-1 (figure 1B) and one exemplary Gal-3 (figure 1C) pull-down experiment. Those proteins, that could be detected in 2 or more independent experiments (FC≥2, $p<0.05$, n≥2) were determined as the most significant potential interactors of Gal-1 and Gal-3 (figure 1A, right). 131 Gal-3 interactors and 15 Gal-1 interactors fulfilling these strict criteria were used for further analysis and validation (table 1 and table 2).

ASBMB MOLECULAR & CELLULAR PROTEOMICS MCP

**Galectin-1 and Galectin-3 interactors play a role in multiple binding processes and are mainly localized in membranes**

GeneRanker analysis of the 131 Gal-3 and the 15 Gal-1 interacting proteins based on the GeneOntology (GO) term "cellular component" (supplemental tableS1) and visualized by FunRich classifications[64] revealed that both, Gal-1 and Gal-3 interactors, were mainly localized in membranes (figure 2A). Gal-3 interactors are represented on the outer ring in figure 2A, Gal-1 interactors on the inner ring, illustrating that classifications to subcellular localizations of interactors of both galectins are equally spread. Phobius analysis assigned 9 of the 15 Gal-1 interactors and 71 Gal-3 interactors to have at least one transmembrane domain (table 1 and table 2). Based on GeneRanker analysis, 7 Gal-1 interactors and 67 of the 131 identified Gal-3 interactors are localized to the plasma membrane or on the cell surface. Gal-1 and Gal-3 interactors were also analyzed by the GO term "molecular functions" (supplemental tableS1) and clustered based on this term in the Cytoscape ClueGo-CluePedia[65] network (figures 2B and 2C). Figure 2B and 2C show that Gal-1 and Gal-3 interactors play a role in multiple binding processes. Whereas Gal-1 interactors are involved in integrin, collagen and fibronectin binding processes (figure 2B), Gal-3 interactors comprise functions like glycosaminoglycan and growth factor binding among others (figure 2C). With this approach, we could identify known Gal-3 interactors like for example LAMP1, BSG or different members of the integrin family. Two novel identified interactors of great interest are the low density lipoprotein receptor-related protein 1 (LRP1) and the platelet-derived growth factor receptor beta (PDGFRB). LRP1 is an endocytotic receptor involved in processes of cell migration and invasion, as well as in the regulation of growth factor homeostasis[68-71] and is overexpressed in RPE and RMG cells in PVR[71]. In this pull-down approach, enrichment factors of LRP1 of 31.1 as Gal-1 interactor and of 41.5 as Gal-3 interactor could be identified (table 1 and table 2), which lead to the hypothesis, that LRP1 could be a context-relevant ligand for both galectins. LRP1 also associates with the PDGF

receptor in endosomal compartments and modulates its signaling properties affecting the MAPK and Akt/phosphatidylinositol 3-kinase pathways[72]. PDGF and PDGFR are key regulators of cell migration and proliferation and play a significant role in PVR development[73]. PDGFRB could be identified as Gal-3 interactor with an enrichment factor of 11.7. In order to validate LRP1 and PDGFRB as potential targets for Gal-1 and Gal-3 further functional experiments were performed.

**Galectin-1 induces cross-linking of LRP1, Galectin-3 induces cross-linking of LRP1 and PDGFRB including ITGB1 on the surface of retinal pigment epithelial cells**

It is known that Gal-1 and Gal-3 can cross-link and cluster transmembrane glycoproteins and additionally reduce their mobility[11, 14, 15]. Dynamic lattices on the cell surface are built and several cellular processes can be influenced[14, 15]. In order to check if Gal-1 and Gal-3 are able to cross-link with LRP1 and PDGFRB as well as with the known galectin interactor ITGB1, mesenchymal human RPE cells were treated with biotinylated Gal-1 or Gal-3 for 30 minutes before fixation. The fixed cells were stained with streptavidin coupled Alexa488 to visualize galectin binding and subsequently with the respective antibodies against LRP1, PDGFRB and ITGB1. Immunofluorescence analysis revealed large speckle staining patterns of both galectins (figures 3B and 3C), LRP1 (figures 3E and 3F) and ITGB1 (figures 3H and 3I) in cells treated with Gal-1 and Gal-3 compared to diffuse staining patterns in untreated cells (figures 3A, 3D, 3G). Visualization of double staining with Gal-1/Gal-3 and LRP1 as well as with Gal-1/Gal-3 and ITGB1 indicated a clear overlay of both staining patterns, visible by white (figures 3K and 3L) and yellow (figures 3N and 3O) speckles. Additionally, Gal-1 and Gal-3 induced cross-linking of LRP1 and ITGB1, verified by clear overlay of the respective galectin, LRP1 and ITGB1 staining patterns (white speckles, figures 3Q and 3R). Cross-linking of Gal-3 with PDGFRB and ITGB1 could also be verified (supplemental figure 2). Whereas exogenous galectin treatment resulted



ASBMB MOLECULAR & CELLULAR PROTEOMICS MCP

ASBMB MOLECULAR & CELLULAR PROTEOMICS MCP

in clear co-localization of LRP1/PDGFRB and ITGB1 on the cell surface of human RPE cells, no obvious cluster formation could be seen without addition of exogenous galectin (figures 3J, 3M and 3P).

**Binding of Galectin-1 and Galectin-3 on LRP1 and PDGFRB is glycosylation-dependent**

Crucial for galectin-binding and lattice formation are the number of glycoprotein ligands and the branching of their N-glycans[74]. In detail, the amount and the branching of N-acetyllactosamine (LacNAc) residues in the glycan pattern are decisive for affinity. In order to find out, whether binding and cross-linking of Gal-1 and Gal-3 with LRP1 and PDGFRB are dependent on specific glycan structures, human RPE cells were treated for up to 4 weeks with 10µM Kifunensine to prevent complex-type N1,6 glycosylation of proteins. Kifunensine is a potent and selective inhibitor of Golgi-class I α-mannosidases [75-77]. When it is added to cell culture medium at concentrations of 4mM or higher, a complete shift of N-glycan patterns from complex structures to Man9(GlcNAc)2 is induced[76, 77]. Galectin-pull down experiments were repeated with RPE cell lysates of cells, treated with or without 10µM Kifunensine. Western Blot analysis revealed that LRP1 and PDGFRB bound weaker to Gal-1 and Gal-3 when cells were treated with Kifunensine (figure 4). This indicates that complex-type N-glycosylation of LRP1 and PDGFRB is necessary for galectin-binding. Inhibition of complex-type-N-glycosylation led also to less galectin binding on the cell surface (figure 5A and 5C) and no cross-linking of the respective galectins with LRP1 (figure 5A4 and 5C4), PDGFRB (supplemental figure 3I) and ITGB1 (figure 5A3 and 5A3) was induced, in contrast to the untreated cells as described before.

**Enhanced phosphorylation of ERK-1/2 and AKT-1/2/3 by binding of Gal-1 and Gal-3**

To analyze functional and signal modulating effects of galectins on RPE cells, simultaneous screening of changes in phosphorylation profiles in response to galectin binding was performed.

ASBMB MOLECULAR & CELLULAR PROTEOMICS MCP

ARPE-19 cells were untreated or treated with Gal-1 and Gal-3 for 1, 15 or 30 minutes. Both Gal-1 and Gal-3 treatment significantly enhanced phosphorylation of the extracellular signal regulated kinase ERK-1/2 and the serine-threonine protein kinase AKT-1/2/3 (S473) (figure 6A). ERK-1 was phosphorylated at the threonine residue T202 and at the tyrosine residue Y204, ERK-2 at T185 and Y187. The corresponding Western Blot analysis (figure 6B) showed that phosphorylation of ERK1/2 was already enhanced after one minute Gal-1 and Gal-3 treatment and was still detectable after 30 minutes. Phosphorylation of glycogen synthase kinase GSK-3α/β (S21/S9) and proline-rich protein Pras-40 (T246) were also induced by galectin treatment (figure 6A).

ASBMB MOLECULAR & CELLULAR PROTEOMICS MCP

## Discussion

This study was designed to identify specific interactors for Gal-1 and Gal-3 on mesenchymal RPE cell surfaces to get deeper insight in the functional effects of galectins on RPE cells in context of PVR. For interactome screening we used whole cell extracts of cultured human RPE cells that dedifferentiated and transformed into a fibroblast-like phenotype under the used cell culture conditions. Cultivation of RPE cells on plastic in the presence of serum is a widely accepted in vitro model system for early PVR[27] and since we wanted to identify galectin interactors on RPE cells mimicking status of early PVR we used primary human RPE cells of nine different human donors. Besides, the human ARPE-19 cell line is often used in RPE cell research[55, 78]. In this approach, we used them for the analysis of signal modulating effects of galectins on RPE cells due to the required high amount of whole cell extracts.

Gal-1 and Gal-3 pull-down experiments and subsequent quantitative LC-MSMS analysis with strict filtering to avoid unspecific binders resulted in a total of 131 significant Gal-3 interacting binding partners while only 15 proteins remained as significant Gal-1 ligands. The unequal number of interactors can be explained by structural differences of Gal-1 and Gal-3 in their CRD domains. Gal-3 is the only known chimera type galectin and it cross-links glycoproteins by its C-terminal domain and multimerizes by its N-terminal domain after binding to saccharide ligands[9, 11]. In contrast to that, Gal-1 consists of one CRD and can form homodimers by its N-terminal domain[12, 13, 16, 17]. By coupling of galectins to sepharose beads, physiological multimerization is presumably hindered and this conformation change might influence the ability of the CRD domain to bind glycoproteins. However, the binding activity of Gal-1 and Gal-3 after coupling to the beads was confirmed by incubation with asialofetuin, a known interactor via β-galactoside moieties (supplemental figure 1). In vivo, ligand binding occurs at the CRD domain while multimerization of galectins and formation of cross-linked lattices is triggered by the N-terminal

ASBMB MOLECULAR & CELLULAR PROTEOMICS MCP

domain (figures 3 and 5)[11, 79]. Consequently, multimerization is in vivo not important for recognition of specific ligands and coupling of galectins to beads should not generally hinder identification of galectin interactors. However, we can't exclude a different behavior of Gal-1 and Gal-3 with respect to forced monomerization through bead coupling, but Gal-1 and Gal-3 pull-down experiments were done in parallel under the same conditions with the same RPE cell lysates and multimerization is at least equally important for Gal-3 as compared to Gal-1. Thus, we assume that the lower numbers of Gal-1 interactors are not due to technical limitations, but rather reflect a reduced spectrum of interactors. In vivo, the pentameric form of Gal-3 may facilitate to bind more different glycoprotein receptors on the RPE cell surface. Stillman et al. [40] showed for instance, that lower concentrations of Gal-3 are required to trigger T cell death than of Gal-1, suggesting that Gal-3 is able to bind more ligands simultaneously. Even though all members of the galectin family bind to galactose-β1,4-N-acetylglucosamine, it is assumed that the structural differences in their CRD domains not only lead to different specificities for distinct glycoproteins, but also to distinct biological activities[40, 80, 81]. Whereas Gal-3 for example is associated with antiapoptotic effects, Gal-1 induces apoptosis in several cell types [82, 83]. On the other hand, binding to different interactors does not necessarily mean that different downstream mechanisms are influenced. In the literature it is shown that Gal-1 and Gal-3 can bind to distinct receptors but converge on similar downstream signaling in several analyses for induction of T cell death[40] or of neutrophil respiratory burst[84, 85]. This assumption is further underscored by the finding that Gal-1 and Gal-3 don't show synergistic effects with respect to inhibition of RPE cell attachment and spreading when added simultaneously[30].

Nevertheless, the identified Gal-1 and Gal-3 interactors have many common features. They are distributed in the same cellular components, mainly in membranes, and play a role in multiple binding processes (figure 2). Analysis of galectin-interactors in whole RPE cell lysates with combined pull-down experiments and quantitative MS screening revealed both intra- and

ASBMB MOLECULAR & CELLULAR PROTEOMICS MCP

extracellular interactors. It is known, that Gal-1 and Gal-3 are present both inside and outside the cell, and that Gal-1 and Gal-3 interact also with intracellular proteins. For example, they are involved in processes like pre-mRNA splicing[86, 87], but these processes are assumed to be based on protein-protein interactions rather than carbohydrate-lectin interactions on the cell surface or extracellular matrix (ECM)[88]. In this approach, interacting proteins were eluted with ß-lactose to verify carbohydrate-dependent binding on Galectins. Thus, we are focusing on the Gal-1 and Gal-3 interactors on cell-surface and ECM. Seven Gal-1 interactors and 67 of the 131 identified Gal-3 interactors are localized in plasma membrane or on the cell surface, based on GeneRanker analysis. Figure 2A shows the distribution of the identified interactors on cellular components. Most of the interactors are localized in membranes, the extracellular space or intraluminal, validating that this approach mainly pulled down the carbohydrate-dependent interacting ligands. GeneRanker analysis also showed that both Gal-1 and Gal-3 interactors are involved in cell adhesion processes (supplemental table 2). Gal-3 interactors also play a role in ECM organization and cell migration, while Gal-1 interactors are involved in integrin-mediated signaling pathways. With respect to PVR, these biological processes are the key cellular processes in disease development, which is characterized by adhesion, migration and EMT of RPE and RMG cells[20, 23, 25]. The data monitored by our gene ranker analysis are of particular interest since target proteins of both Gal-1 and Gal-3 may play a role in the pathogenesis of PVR and thus be instrumental for influencing the disease process in terms of a therapeutic approach. From recent studies it became evident that PVR is a multifactorial cellular process that can't be attenuated by inhibition of single growth factors and their downstream signaling pathways or by anti-inflammatory or anti-proliferative approaches alone[32-39]. As seen from our data, Gal-1 and Gal-3 may have the ability to orchestrate several cellular processes involved in PVR development simultaneously by interacting with a variety of distinct cell surface interactors, and thus provide a multimodal therapeutic concept.

ASBMB MOLECULAR & CELLULAR PROTEOMICS MCP

Most galectin ligands are branched N-glycans on transmembrane proteins[89]. Accordingly, we found that complex-type-N-glycosylation of the galectin interactors LRP1 and PDGFRB is required for galectin-binding and lattice formation on the RPE cell surface (figures 4 and 5). Of note, these glycans are upregulated during EMT of human RPE cells and these changes lead to increased binding of Gal-3 to mesenchymal RPE cells[31]. Consequently it can be assumed that EMT sensitizes the susceptibility of cell surface receptors to galectins and that complex-type-N-glycan structures are very important for galectin binding. Analyzing the mechanisms of these glycan-galectin interactions will provide evidence whether these glycan structures are a prerequisite for galectin binding and how they influence interaction processes.

Several galectin interactors in different cell types are known so far[90]. Gal-3 interacts for instance with EGFR and TGF-βR in tumor cells[45, 91]. Both, Gal-1 and Gal-3, bind to β1-integrins[42, 92, 93] and extracellular matrix molecules like fibronectin and laminin[52, 94, 95]. Besides, Gal-1 and Gal-3 can also bind to immune cell glycoproteins and to neural recognition molecules[40, 43, 82, 96-99]. ITGB1 and CD147 (BSG), the two previously identified counter-receptors for Gal-3 in RPE cells were confirmed with this approach[42]. Additionally, known interactors of Gal-1 or Gal-3 like laminin[52, 94], LAMP1 and LAMP2[100] and integrins[101] among others were confirmed. Most of these interactors were identified in distinct cell types, but not in RPE cells. Thus we could on the one hand confirm several of the known interactors in RPE cells, and on the other hand identify many new so far unknown interactors.

For validation we focused on two novel identified Gal-1 and Gal-3 interactors: LRP1 and PDGFRB. LRP1 (or CD91) is a 600kDa glycoprotein, consisting of an extracellular and a transmembrane domain[102, 103]. LRP1 recognizes at least 30 different ligands, among others lipoproteins[104], the β-amyloid precursor protein[68], and the protease inhibitor α2-macroglobulin (α2M), which is responsible for the clearance of several growth factors and cytokines like for

ASBMB MOLECULAR & CELLULAR PROTEOMICS MCP

example TGF-β[105-107]. LRP1 recognizes extracellular ligands and induces endocytosis for degradation by lysosomes[70]. Thus, it is assumed that LRP1 also plays a significant role in the clearance of α2-M-associated growth factors and could potentially be involved in pathologic events during PVR development[71]. Hollborn et al. [71] found that LRP1 mRNA levels are upregulated in human RPE cells, stimulated with TGF-β1, TGF-β2 or VEGF. They hypothesize that protease treatment aiming to induce α2M-mediated clearance of growth factors accompanied by increased LRP1-mediated endocytosis is a potential treatment strategy for PVR[71]. Yet, in PVR RPE and RMG cells are exposed to high amounts of growth factors and cytokines. Though Milenkovic et al. [108] found that α2M inhibited RMG cell proliferation, it remains unclear, whether it is possible to clear most of these growth factors by α2M activation or by intravitreal addition of α2M. It is also known that several signaling pathways - including ERK/MAPK, Akt and NF-κB - are activated by binding of α2M to LRP1 in distinct cell types including macrophages and RMG cells. Bonacci et al. [109] found that proliferation and MAPK-ERK1/2 activation in a macrophage-derived cell-line is induced by binding of α2M to LRP1. They could verify that α2M promotes expression and secretion of matrix-metalloproteinase MMP-9, which was also mediated by MAPK-ERK1/2 and NF- κB[110]. α2M activates also GFAP expression in RMG cells induced by LRP1, which is assumed to be mediated by the JAK/STAT signaling pathway[111]. Barcelona et al. [112] found that α2M - mediated by LRP1 - induces RMG cell migration by regulating MT1-MMP activity. We show here that α2M is a significant Gal-3 interactor with an enrichment factor over 30.9 and a p-value of 0.002 (table 2). Which effect binding of Gal-1 and Gal-3 on LRP1 or α2M has on cellular processes of RPE cells, remains to be solved. Interestingly, LRP1 can be tyrosine phosphorylated by the growth factor PDGFR, which in turn regulates its activity by endocytosis and intracellular trafficking of LRP1[113-115]. Thus, LRP1 is predicted to interact as a co-receptor that modulates PDGFR initiated signal transduction pathways, like for example the control of cell migration[113-115]. In depth

ASBMB MOLECULAR & CELLULAR PROTEOMICS MCP

characterization of downstream signals influenced by Gal-1 and Gal-3 interaction with the identified glycan-dependent interactors will provide more insight how galectins modify RPE cell behavior. By simultaneous screening of changes in phosphorylation profiles of distinct protein kinases, we could show that both ERK/MAPK and Akt signaling pathways are affected by galectin binding (figure 6). ERK phosphorylation was stable up to 30 minute after galectin treatment. Akt, which is also called protein kinase B, is one of the main downstream targets of the phosphatidylinositol (PI) 3-kinase pathway[116, 117]. GSK-3α/β and Pras-40 are substrates of Akt[116-118] and accordingly, both were also phosphorylated after galectin treatment. Since it is known that LRP1 and PDGFRB associate in endosomal compartments and affect MAPK and Akt/PI 3-kinase pathways[72], we assume that galectin induced cluster formation of LRP1, ITGB1 and PDGFRB on the cell surface have an influence on those signaling pathways in RPE cells. Interestingly, Gal-1 also induced clustering of PDGFRB and ITGB1 (data not shown), even though PDGFRB was not identified as Gal-1 interactor by the pull-down experiments, giving a hint that Gal-1 not only forms lattices with specific interactors, but larger interacting protein complexes might be included. The experimental set-up with the galectin pull-down assays results in an initial set of galectin interactors, but does not allow to distinguish between direct and indirect galectin interactors, which is a general problem in interactome studies based on pull-down approaches. In vivo, Gal-1 and Gal-3 interact due to their multimerization with several glycoproteins simultaneously and formation of cross-linked lattices takes place. In many biological systems, it is described that clustering of ordered arrays of galectins and their glycoprotein ligands on the cell surface is required for cellular signaling and adhesion processes. The interplay between the different ligands – direct or indirect – is very important to get deeper insights in the functional effects of galectins on RPE cells.

In conclusion, not only known interactors of Gal-1 and Gal-3 were confirmed, but also many novel interactors could be detected in this first proteome-wide comprehensive Gal-1 and Gal-3

ASBMB
MOLECULAR & CELLULAR PROTEOMICS
MCP

interactome screening. Two of the identified interactors, namely LRP1 and PDGFRB, could be validated as Gal-1 and Gal-3 interactors by showing that exogenously added Gal-1 and Gal-3 induce cross-linking on the RPE cell surface with LRP1 and PDGFRB together with the transmembrane protein ITGB1 in a complex-type N-glycan-binding-dependent manner.

ASBMB MOLECULAR & CELLULAR PROTEOMICS MCP

**Acknowledgment**

The authors would like to thank Nicole Senninger, Jennifer Behler and Fabian Gruhn for excellent technical assistance and Uli Ohmayer and Christine von Törne for helpful discussions. This work was supported by grants from the Deutsche Forschungsgemeinschaft – DFG: grant no HA6014/2-2 to SMH and grant no PR 1248/2-2 to CSP.

ASBMB MOLECULAR & CELLULAR PROTEOMICS MCP

## References


[1] Barondes, S., Castronovo, V., Cooper, D. N., Cummings, R. D., Drickamer, K., Feizi, T., Gitt, M., Hirabayashi, J., Hughes, C., and Kasai, K. (1994) Galectins: a family of animal pgalactoside-binding lectins, *Cell 76*, 597-598.

[2] Cooper, D. N., and Barondes, S. H. (1999) God must love galectins; he made so many of them, *Glycobiology 9*, 979-984.

[3] Hirabayashi, J., and Kasai, K.-i. (1993) The family of metazoan metal-independent β-galactoside-binding lectins: structure, function and molecular evolution, *Glycobiology 3*, 297-304.

[4] Cooper, D. N. (2002) Galectinomics: finding themes in complexity, *Biochimica et Biophysica Acta (BBA)-General Subjects 1572*, 209-231.

[5] Römer, C. E., and Elling, L. (2011) *Galectins: Structures, binding properties and function in cell adhesion*, INTECH Open Access Publisher.

[6] Gabius, H.-J. (2011) *The sugar code: fundamentals of glycosciences*, John Wiley & Sons.

[7] Hughes, R. C. (2001) Galectins as modulators of cell adhesion, *Biochimie 83*, 667-676.

[8] Elola, M., Wolfenstein-Todel, C., Troncoso, M., Vasta, G., and Rabinovich, G. (2007) Galectins: matricellular glycan-binding proteins linking cell adhesion, migration, and survival, *Cellular and Molecular Life Sciences 64*, 1679-1700.

[9] Gabius, H. J. (1997) Animal lectins, *European Journal of Biochemistry 243*, 543-576.

[10] Leffler, H., Carlsson, S., Hedlund, M., Qian, Y., and Poirier, F. (2002) Introduction to galectins, *Glycoconjugate journal 19*, 433-440.

[11] Ahmad, N., Gabius, H.-J., André, S., Kaltner, H., Sabesan, S., Roy, R., Liu, B., Macaluso, F., and Brewer, C. F. (2004) Galectin-3 precipitates as a pentamer with synthetic multivalent carbohydrates and forms heterogeneous cross-linked complexes, *Journal of Biological Chemistry 279*, 10841-10847.

[12] Cho, M., and Cummings, R. D. (1997) Galectin-1: oligomeric structure and interactions with polylactosamine, *Trends in Glycoscience and Glycotechnology 9*, 47-56.

[13] Lobsanov, Y. D., Gitt, M., Leffler, H., Barondes, S., and Rini, J. (1993) X-ray crystal structure of the human dimeric S-Lac lectin, L-14-II, in complex with lactose at 2.9-A resolution, *Journal of Biological Chemistry 268*, 27034-27038.

[14] Fred Brewer, C. (2002) Binding and cross-linking properties of galectins, *Biochimica et Biophysica Acta (BBA) - General Subjects 1572*, 255-262.

[15] Brewer, C. F. (1997) Cross-linking activities of galectins and other multivalent lectins, *Trends in Glycoscience and Glycotechnology 9*, 155-165.

[16] Bourne, Y., Bolgiano, B., Liao, D.-I., Strecker, G., Cantau, P., Herzberg, O., Feizi, T., and Cambillau, C. (1994) Crosslinking of mammalian lectin (galectin-1) by complex biantennary saccharides, *Nature Structural & Molecular Biology 1*, 863-870.

[17] Gupta, D., and Brewer, C. F. (1994) Homogeneous Aggregation of the 14-kDa. beta.-Galactoside Specific Vertebrate Lectin Complex with Asialofetuin in Mixed Systems, *Biochemistry 33*, 5526-5530.

[18] Committee, R. S. T. (1983) The classification of retinal detachment with proliferative vitreoretinopathy, *Ophthalmology 90*, 121-125.

[19] Cardillo, J. A., Stout, J. T., LaBree, L., Azen, S. P., Omphroy, L., Cui, J. Z., Kimura, H., Hinton, D. R., and Ryan, S. J. (1997) Post-traumatic Proliferative Vitreoretinopathy, *Ophthalmology 104*, 1166-1173.

ASBMB MOLECULAR & CELLULAR PROTEOMICS MCP

[20] Machemer, R. (1988) Proliferative vitreoretinopathy (PVR): a personal account of its pathogenesis and treatment, *Investigative ophthalmology & visual science 29*, 1771-1783.
[21] Pastor, J. C. (1998) Proliferative vitreoretinopathy: an overview, *Survey of ophthalmology 43*, 3-18.
[22] Kampik, A., Kenyon, K. R., Michels, R. G., Green, W. R., and Zenaida, C. (1981) Epiretinal and vitreous membranes: comparative study of 56 cases, *Archives of ophthalmology 99*, 1445-1454.
[23] Machemer, R. (1978) Pathogenesis and classification of massive periretinal proliferation, *British Journal of Ophthalmology 62*, 737-747.
[24] Pastor, J. C., de la Rúa, E. R. g., and Martín, F. (2002) Proliferative vitreoretinopathy: risk factors and pathobiology, *Progress in Retinal and Eye Research 21*, 127-144.
[25] Hiscott, P., Sheridan, C., Magee, R. M., and Grierson, I. (1999) Matrix and the retinal pigment epithelium in proliferative retinal disease, *Progress in retinal and eye research 18*, 167-190.
[26] Yang, S., Li, H., Li, M., and Wang, F. (2015) Mechanisms of epithelial-mesenchymal transition in proliferative vitreoretinopathy, *Discovery medicine 20*, 207-217.
[27] Grisanti, S., and Guidry, C. (1995) Transdifferentiation of retinal pigment epithelial cells from epithelial to mesenchymal phenotype, *Investigative ophthalmology & visual science 36*, 391-405.
[28] Hughes, R. C. (1999) Secretion of the galectin family of mammalian carbohydrate-binding proteins, *Biochimica et Biophysica Acta (BBA)-General Subjects 1473*, 172-185.
[29] Alge-Priglinger, C. S., André, S., Kreutzer, T. C., Deeg, C. A., Kampik, A., Kernt, M., Schöffl, H., Priglinger, S. G., and Gabius, H.-J. (2009) Inhibition of human retinal pigment epithelial cell attachment, spreading, and migration by the human lectin galectin-1.
[30] Alge-Priglinger, C. S., André, S., Schoeffl, H., Kampik, A., Strauss, R. W., Kernt, M., Gabius, H.-J., and Priglinger, S. G. (2011) Negative regulation of RPE cell attachment by carbohydrate-dependent cell surface binding of galectin-3 and inhibition of the ERK–MAPK pathway, *Biochimie 93*, 477-488.
[31] Priglinger, C. S., Obermann, J., Szober, C. M., Merl-Pham, J., Ohmayer, U., Behler, J., Gruhn, F., Kreutzer, T. C., Wertheimer, C., and Geerlof, A. (2016) Epithelial-to-Mesenchymal Transition of RPE Cells In Vitro Confers Increased [Beta] 1, 6-N-Glycosylation and Increased Susceptibility to Galectin-3 Binding, *PloS one 11*.
[32] Pennock, S., Rheaume, M.-A., Mukai, S., and Kazlauskas, A. (2011) A novel strategy to develop therapeutic approaches to prevent proliferative vitreoretinopathy, *The American journal of pathology 179*, 2931-2940.
[33] Velez, G., Weingarden, A. R., Lei, H., Kazlauskas, A., and Gao, G. (2013) SU9518 Inhibits Proliferative Vitreoretinopathy in Fibroblast and Genetically Modified Müller Cell–Induced Rabbit Models, *Investigative ophthalmology & visual science 54*, 1392-1397.
[34] Priglinger, C., and Priglinger, S. (2013) [Pharmacological approach to treatment of proliferative vitreoretinopathy], *Der Ophthalmologe: Zeitschrift der Deutschen Ophthalmologischen Gesellschaft 110*, 948-959.
[35] Wiedemann, P., Hilgers, R., Bauer, P., Heimann, K., and Group, D. S. (1998) Adjunctive daunorubicin in the treatment of proliferative vitreoretinopathy: results of a multicenter clinical trial, *American journal of ophthalmology 126*, 550-559.
[36] Charteris, D. G., Aylward, G. W., Wong, D., Groenewald, C., Asaria, R. H. Y., and Bunce, C. (2004) A randomized controlled trial of combined 5-fluorouracil and low-molecular-weight heparin in management of established proliferative vitreoretinopathy, *Ophthalmology 111*, 2240-2245.
[37] Turgut, B., Uyar, F., Ustundag, B., Celiker, U., Akpolat, N., and Demir, T. (2012) The impact of tacrolimus on growth factors in experimental proliferative vitreoretinopathy, *Retina 32*, 232-241.

ASBMB MOLECULAR & CELLULAR PROTEOMICS MCP

[38] Kita, T., Hata, Y., Arita, R., Kawahara, S., Miura, M., Nakao, S., Mochizuki, Y., Enaida, H., Goto, Y., and Shimokawa, H. (2008) Role of TGF-β in proliferative vitreoretinal diseases and ROCK as a therapeutic target, *Proceedings of the National Academy of Sciences 105*, 17504-17509.
[39] Zheng, Y., Ikuno, Y., Ohj, M., Kusaka, S., Jiang, R., Çekiç, O., Sawa, M., and Tano, Y. (2003) Platelet-derived Growth Factor Receptor Kinase Inhibitor AG1295 and Inhibition of Experimental Proliferative Vitreoretinopathy, *Japanese Journal of Ophthalmology 47*, 158-165.
[40] Stillman, B. N., Hsu, D. K., Pang, M., Brewer, C. F., Johnson, P., Liu, F.-T., and Baum, L. G. (2006) Galectin-3 and galectin-1 bind distinct cell surface glycoprotein receptors to induce T cell death, *The Journal of Immunology 176*, 778-789.
[41] Yu, L.-G., Andrews, N., Zhao, Q., McKean, D., Williams, J. F., Connor, L. J., Gerasimenko, O. V., Hilkens, J., Hirabayashi, J., and Kasai, K. (2007) Galectin-3 interaction with Thomsen-Friedenreich disaccharide on cancer-associated MUC1 causes increased cancer cell endothelial adhesion, *Journal of Biological Chemistry 282*, 773-781.
[42] Priglinger, C. S., Szober, C. M., Priglinger, S. G., Merl, J., Euler, K. N., Kernt, M., Gondi, G., Behler, J., Geerlof, A., and Kampik, A. (2013) Galectin-3 induces clustering of CD147 and integrin-β1 transmembrane glycoprotein receptors on the RPE cell surface, *PloS one 8*, e70011.
[43] Probstmeier, R., Montag, D., and Schachner, M. (1995) Galectin-3, a β-Galactoside-Binding Animal Lectin, Binds to Neural Recognition Molecules, *Journal of neurochemistry 64*, 2465-2472.
[44] Markowska, A. I., Jefferies, K. C., and Panjwani, N. (2011) Galectin-3 protein modulates cell surface expression and activation of vascular endothelial growth factor receptor 2 in human endothelial cells, *Journal of Biological Chemistry 286*, 29913-29921.
[45] Partridge, E. A., Le Roy, C., Di Guglielmo, G. M., Pawling, J., Cheung, P., Granovsky, M., Nabi, I. R., Wrana, J. L., and Dennis, J. W. (2004) Regulation of cytokine receptors by Golgi N-glycan processing and endocytosis, *Science 306*, 120-124.
[46] Rapoport, E., Kurmyshkina, O., and Bovin, N. (2008) Mammalian galectins: structure, carbohydrate specificity, and functions, *Biochemistry (Moscow) 73*, 393-405.
[47] Markowska, A. I., Liu, F.-T., and Panjwani, N. (2010) Galectin-3 is an important mediator of VEGF- and bFGF-mediated angiogenic response, *The Journal of experimental medicine 207*, 1981-1993.
[48] Pace, K. E., Lee, C., Stewart, P. L., and Baum, L. G. (1999) Restricted receptor segregation into membrane microdomains occurs on human T cells during apoptosis induced by galectin-1, *The Journal of Immunology 163*, 3801-3811.
[49] Dumic, J., Dabelic, S., and Flögel, M. (2006) Galectin-3: an open-ended story, *Biochimica et Biophysica Acta (BBA)-General Subjects 1760*, 616-635.
[50] Dong, S., and Hughes, R. C. (1997) Macrophage surface glycoproteins binding to galectin-3 (Mac-2-antigen), *Glycoconjugate journal 14*, 267-274.
[51] Furtak, V., Hatcher, F., and Ochieng, J. (2001) Galectin-3 mediates the endocytosis of β-1 integrins by breast carcinoma cells, *Biochemical and biophysical research communications 289*, 845-850.
[52] Kuwabara, I., and Liu, F.-T. (1996) Galectin-3 promotes adhesion of human neutrophils to laminin, *The Journal of Immunology 156*, 3939-3944.
[53] Ochieng, J., Leite-Browning, M. L., and Warfield, P. (1998) Regulation of cellular adhesion to extracellular matrix proteins by galectin-3, *Biochemical and biophysical research communications 246*, 788-791.
[54] Alberts, B., Johnson, A., Lewis, J., Walter, P., Raff, M., and Roberts, K. (2002) Molecular Biology of the Cell 4th Edition: International Student Edition, Routledge.
[55] Kuznetsova, A. V., Kurinov, A. M., and Aleksandrova, M. A. (2014) Cell models to study regulation of cell transformation in pathologies of retinal pigment epithelium, *Journal of ophthalmology 2014*.

ASBMB MOLECULAR & CELLULAR PROTEOMICS MCP

[56] Nowak, T., Haywood, P., and Barondes, S. (1976) Developmentally regulated lectin in embryonic chick muscle and a myogenic cell line, *Biochemical and biophysical research communications 68*, 650-657.
[57] St-Pierre, C., Ouellet, M., Giguère, D., Ohtake, R., Roy, R., Sato, S., and Tremblay, M. J. (2012) Galectin-1-specific inhibitors as a new class of compounds to treat HIV-1 infection, *Antimicrobial agents and chemotherapy 56*, 154-162.
[58] Wisniewski, J. R., Zougman, A., Nagaraj, N., and Mann, M. (2009) Universal sample preparation method for proteome analysis, *Nature methods 6*, 359.
[59] Hauck, S. M., Dietter, J., Kramer, R. L., Hofmaier, F., Zipplies, J. K., Amann, B., Feuchtinger, A., Deeg, C. A., and Ueffing, M. (2010) Deciphering membrane-associated molecular processes in target tissue of autoimmune uveitis by label-free quantitative mass spectrometry, *Molecular & Cellular Proteomics 9*, 2292-2305.
[60] Merl, J., Deeg, C. A., Swadzba, M. E., Ueffing, M., and Hauck, S. M. (2013) Identification of autoantigens in body fluids by combining pull-downs and organic precipitations of intact immune complexes with quantitative label-free mass spectrometry, *Journal of proteome research 12*, 5656-5665.
[61] Grosche, A., Hauser, A., Lepper, M. F., Mayo, R., von Toerne, C., Merl-Pham, J., and Hauck, S. M. (2015) The proteome of native adult Muller glial cells from murine retina, *Molecular & Cellular Proteomics*, mcp. M115. 052183.
[62] Ly, A., Merl-Pham, J., Priller, M., Gruhn, F., Senninger, N., Ueffing, M., and Hauck, S. M. (2016) Proteomic profiling suggests central role of STAT signaling during retinal degeneration in the rd10 mouse model, *Journal of proteome research 15*, 1350-1359.
[63] Vizcaíno, J. A., Csordas, A., del-Toro, N., Dianes, J. A., Griss, J., Lavidas, I., Mayer, G., Perez-Riverol, Y., Reisinger, F., and Ternent, T. (2016) 2016 update of the PRIDE database and its related tools, *Nucleic acids research 44*, D447-D456.
[64] Pathan, M., Keerthikumar, S., Ang, C. S., Gangoda, L., Quek, C. Y., Williamson, N. A., Mouradov, D., Sieber, O. M., Simpson, R. J., and Salim, A. (2015) FunRich: An open access standalone functional enrichment and interaction network analysis tool, *Proteomics 15*, 2597-2601.
[65] Bindea, G., Mlecnik, B., Hackl, H., Charoentong, P., Tosolini, M., Kirilovsky, A., Fridman, W.-H., Pagès, F., Trajanoski, Z., and Galon, J. (2009) ClueGO: a Cytoscape plug-in to decipher functionally grouped gene ontology and pathway annotation networks, *Bioinformatics 25*, 1091-1093.
[66] Käll, L., Krogh, A., and Sonnhammer, E. L. (2004) A combined transmembrane topology and signal peptide prediction method, *Journal of molecular biology 338*, 1027-1036.
[67] Schneider, C. A., Rasband, W. S., and Eliceiri, K. W. (2012) NIH Image to ImageJ: 25 years of image analysis, *Nature methods 9*, 671.
[68] Kounnas, M. Z., Moir, R. D., Rebeck, G. W., Bush, A. I., Argraves, W. S., Tanzi, R. E., Hyman, B. T., and Strickland, D. K. (1995) LDL receptor-related protein, a multifunctional ApoE receptor, binds secreted β-amyloid precursor protein and mediates its degradation, *Cell 82*, 331-340.
[69] Ulery, P. G., Beers, J., Mikhailenko, I., Tanzi, R. E., Rebeck, G. W., Hyman, B. T., and Strickland, D. K. (2000) Modulation of β-amyloid precursor protein processing by the low density lipoprotein receptor-related protein (LRP) Evidence that LRP contributes to the pathogenesis of Alzheimer's disease, *Journal of Biological Chemistry 275*, 7410-7415.
[70] Li, Y., Lu, W., Marzolo, M. P., and Bu, G. (2001) Differential functions of members of the low density lipoprotein receptor family suggested by their distinct endocytosis rates, *Journal of Biological Chemistry 276*, 18000-18006.

ASBMB MOLECULAR & CELLULAR PROTEOMICS MCP

[71] Hollborn, M., Birkenmeier, G., Saalbach, A., Iandiev, I., Reichenbach, A., Wiedemann, P., and Kohen, L. (2004) Expression of LRP1 in retinal pigment epithelial cells and its regulation by growth factors, *Investigative ophthalmology & visual science 45*, 2033-2038.
[72] Muratoglu, S. C., Mikhailenko, I., Newton, C., Migliorini, M., and Strickland, D. K. (2010) Low density lipoprotein receptor-related protein 1 (LRP1) forms a signaling complex with platelet-derived growth factor receptor-β in endosomes and regulates activation of the MAPK pathway, *Journal of Biological Chemistry 285*, 14308-14317.
[73] Cui, J., Lei, H., Samad, A., Basavanthappa, S., Maberley, D., Matsubara, J., and Kazlauskas, A. (2009) PDGF receptors are activated in human epiretinal membranes, *Experimental eye research 88*, 438-444.
[74] Nabi, I. R., Shankar, J., and Dennis, J. W. (2015) The galectin lattice at a glance, *J Cell Sci 128*, 2213-2219.
[75] Kayakiri, H., Kasahara, C., Oku, T., and Hashimoto, M. (1990) Synthesis of kifunensine, an immunomodulating substance isolated from microbial source, *Tetrahedron letters 31*, 225-226.
[76] Elbein, A. D. (1991) Glycosidase inhibitors: inhibitors of N-linked oligosaccharide processing, *The FASEB Journal 5*, 3055-3063.
[77] Elbein, A. D., Tropea, J. E., Mitchell, M., and Kaushal, G. P. (1990) Kifunensine, a potent inhibitor of the glycoprotein processing mannosidase I, *Journal of Biological Chemistry 265*, 15599-15605.
[78] Kang, G.-Y., Bang, J. Y., Choi, A. J., Yoon, J., Lee, W.-C., Choi, S., Yoon, S., Kim, H. C., Baek, J.-H., and Park, H. S. (2014) Exosomal proteins in the aqueous humor as novel biomarkers in patients with neovascular age-related macular degeneration, *Journal of proteome research 13*, 581-595.
[79] Vijayakumar, S., Peng, H., and Schwartz, G. J. (2013) Galectin-3 mediates oligomerization of secreted hensin using its carbohydrate-recognition domain, *American Journal of Physiology-Renal Physiology 305*, F90-F99.
[80] Kopitz, J., von Reitzenstein, C., André, S., Kaltner, H., Uhl, J., Ehemann, V., Cantz, M., and Gabius, H.-J. (2001) Negative regulation of neuroblastoma cell growth by carbohydrate-dependent surface binding of galectin-1 and functional divergence from galectin-3, *Journal of Biological Chemistry 276*, 35917-35923.
[81] Ahmad, N., Gabius, H.-J., Sabesan, S., Oscarson, S., and Brewer, C. F. (2004) Thermodynamic binding studies of bivalent oligosaccharides to galectin-1, galectin-3, and the carbohydrate recognition domain of galectin-3, *Glycobiology 14*, 817-825.
[82] Pace, K. E., Hahn, H. P., Pang, M., Nguyen, J. T., and Baum, L. G. (2000) Cutting edge: CD7 delivers a pro-apoptotic signal during galectin-1-induced T cell death, *The Journal of Immunology 165*, 2331-2334.
[83] Yang, R.-Y., Hsu, D. K., and LIu, F.-T. (1996) Expression of galectin-3 modulates T-cell growth and apoptosis, *Proceedings of the National Academy of Sciences 93*, 6737-6742.
[84] Almkvist, J., and Karlsson, A. (2002) Galectins as inflammatory mediators, *Glycoconjugate journal 19*, 575-581.
[85] Almkvist, J., Dahlgren, C., Leffler, H., and Karlsson, A. (2002) Activation of the neutrophil nicotinamide adenine dinucleotide phosphate oxidase by galectin-1, *The Journal of Immunology 168*, 4034-4041.
[86] Dagher, S. F., Wang, J. L., and Patterson, R. J. (1995) Identification of galectin-3 as a factor in pre-mRNA splicing, *Proceedings of the National Academy of Sciences 92*, 1213-1217.
[87] Vyakarnam, A., Dagher, S. F., Wang, J. L., and Patterson, R. J. (1997) Evidence for a role for galectin-1 in pre-mRNA splicing, *Molecular and cellular biology 17*, 4730-4737.
[88] Liu, F.-T., and Rabinovich, G. A. (2005) Galectins as modulators of tumour progression, *Nature Reviews Cancer 5*, 29-41.

ASBMB MOLECULAR & CELLULAR PROTEOMICS MCP

[89] Patnaik, S. K., Potvin, B., Carlsson, S., Sturm, D., Leffler, H., and Stanley, P. (2006) Complex N-glycans are the major ligands for galectin-1,-3, and-8 on Chinese hamster ovary cells, *Glycobiology 16*, 305-317.
[90] Boscher, C., Dennis, J. W., and Nabi, I. R. (2011) Glycosylation, galectins and cellular signaling, *Current opinion in cell biology 23*, 383-392.
[91] Lajoie, P., Partridge, E. A., Guay, G., Goetz, J. G., Pawling, J., Lagana, A., Joshi, B., Dennis, J. W., and Nabi, I. R. (2007) Plasma membrane domain organization regulates EGFR signaling in tumor cells, *The Journal of cell biology 179*, 341-356.
[92] Saravanan, C., Liu, F.-T., Gipson, I. K., and Panjwani, N. (2009) Galectin-3 promotes lamellipodia formation in epithelial cells by interacting with complex N-glycans on α3β1 integrin, *Journal of cell science 122*, 3684-3693.
[93] Moiseeva, E. P., Williams, B., Goodall, A. H., and Samani, N. J. (2003) Galectin-1 interacts with β-1 subunit of integrin, *Biochemical and biophysical research communications 310*, 1010-1016.
[94] Moiseeva, E. P., Spring, E. L., Baron, J. H., and de Bono, D. (1999) Galectin 1 modulates attachment, spreading and migration of cultured vascular smooth muscle cells via interactions with cellular receptors and components ofextracellu lar matrix, *Journal of vascular research 36*, 47-58.
[95] Kariya, Y., Kawamura, C., Tabei, T., and Gu, J. (2010) Bisecting GlcNAc residues on laminin-332 down-regulate galectin-3-dependent keratinocyte motility, *Journal of Biological Chemistry 285*, 3330-3340.
[96] Perillo, N. L., Pace, K. E., Seilhamer, J. J., and Baum, L. G. (1995) Apoptosis of T cells mediated by galectin-1.
[97] Hernandez, J. D., Nguyen, J. T., He, J., Wang, W., Ardman, B., Green, J. M., Fukuda, M., and Baum, L. G. (2006) Galectin-1 binds different CD43 glycoforms to cluster CD43 and regulate T cell death, *The Journal of Immunology 177*, 5328-5336.
[98] Walzel, H., Blach, M., Hirabayashi, J., Kasai, K.-I., and Brock, J. (2000) Involvement of CD2 and CD3 in galectin-1 induced signaling in human Jurkat T-cells, *Glycobiology 10*, 131-140.
[99] Fukumori, T., Takenaka, Y., Yoshii, T., Kim, H.-R. C., Hogan, V., Inohara, H., Kagawa, S., and Raz, A. (2003) CD29 and CD7 mediate galectin-3-induced type II T-cell apoptosis, *Cancer research 63*, 8302-8311.
[100] CASTRONOVO, V., WATTIAUX, R., and WATTIAUX-DE CONINCK, S. (1998) Expression of Lamp-1 and Lamp-2 and their interactions with galectin-3 in human tumor cells, *Int. J. Cancer 75*, 105-111.
[101] Gu, M., Wang, W., Song, W. K., Cooper, D., and Kaufman, S. J. (1994) Selective modulation of the interaction of alpha 7 beta 1 integrin with fibronectin and laminin by L-14 lectin during skeletal muscle differentiation, *Journal of cell science 107*, 175-181.
[102] Herz, J., Kowal, R. C., Goldstein, J. L., and Brown, M. S. (1990) Proteolytic processing of the 600 kd low density lipoprotein receptor-related protein (LRP) occurs in a trans-Golgi compartment, *The EMBO journal 9*, 1769.
[103] Herz, J., Hamann, U., Rogne, S., Myklebost, O., Gausepohl, H., and Stanley, K. K. (1988) Surface location and high affinity for calcium of a 500-kd liver membrane protein closely related to the LDL-receptor suggest a physiological role as lipoprotein receptor, *The EMBO journal 7*, 4119.
[104] Beisiegel, U., Weber, W., Ihrke, G., Herz, J., and Stanley, K. K. (1989) The LDL-receptor-related protein, LRP, is an apolipoprotein E-binding protein, *Nature 341*, 162-164.
[105] Kristensen, T., Moestrup, S. K., Gliemann, J., Bendtsen, L., Sand, O., and Sottrup-Jensen, L. (1990) Evidence that the newly cloned low-density-lipoprotein receptor related protein (LRP) is the α2-macroglobulin receptor, *Febs Letters 276*, 151-155.
[106] Strickland, D. K., Ashcom, J., Williams, S., Burgess, W., Migliorini, M., and Argraves, W. S. (1990) Sequence identity between the alpha 2-macroglobulin receptor and low density lipoprotein

ASBMB MOLECULAR & CELLULAR PROTEOMICS MCP

receptor-related protein suggests that this molecule is a multifunctional receptor, *Journal of Biological Chemistry 265*, 17401-17404.

[107] Herz, J., and Strickland, D. K. (2001) LRP: a multifunctional scavenger and signaling receptor, *The Journal of clinical investigation 108*, 779-784.

[108] Milenkovic, I., Birkenmeier, G., Wiedemann, P., Reichenbach, A., and Bringmann, A. (2005) Effect of α2-macroglobulin on retinal glial cell proliferation, *Graefe's Archive for Clinical and Experimental Ophthalmology 243*, 811-816.

[109] Bonacci, G. R., Cáceres, L. C., Sánchez, M. C., and Chiabrando, G. A. (2007) Activated α 2-macroglobulin induces cell proliferation and mitogen-activated protein kinase activation by LRP-1 in the J774 macrophage-derived cell line, *Archives of biochemistry and biophysics 460*, 100-106.

[110] Cáceres, L. C., Bonacci, G. R., Sánchez, M. C., and Chiabrando, G. A. (2010) Activated α2 macroglobulin induces matrix metalloproteinase 9 expression by low-density lipoprotein receptor-related protein 1 through MAPK-ERK1/2 and NF-κB activation in macrophage-derived cell lines, *Journal of cellular biochemistry 111*, 607-617.

[111] Barcelona, P. F., Ortiz, S. G., Chiabrando, G. A., and Sánchez, M. C. (2011) α2-Macroglobulin induces glial fibrillary acidic protein expression mediated by low-density lipoprotein receptor-related protein 1 in Müller cells, *Investigative ophthalmology & visual science 52*, 778-786.

[112] Barcelona, P. F., Jaldín-Fincati, J. R., Sánchez, M. C., and Chiabrando, G. A. (2013) Activated α2-macroglobulin induces Müller glial cell migration by regulating MT1-MMP activity through LRP1, *The FASEB Journal 27*, 3181-3197.

[113] Boucher, P., Gotthardt, M., Li, W.-P., Anderson, R. G., and Herz, J. (2003) LRP: role in vascular wall integrity and protection from atherosclerosis, *Science 300*, 329-332.

[114] Boucher, P., Liu, P., Gotthardt, M., Hiesberger, T., Anderson, R. G., and Herz, J. (2002) Platelet-derived growth factor mediates tyrosine phosphorylation of the cytoplasmic domain of the low density lipoprotein receptor-related protein in caveolae, *Journal of Biological Chemistry 277*, 15507-15513.

[115] Loukinova, E., Ranganathan, S., Kuznetsov, S., Gorlatova, N., Migliorini, M. M., Loukinov, D., Ulery, P. G., Mikhailenko, I., Lawrence, D. A., and Strickland, D. K. (2002) Platelet-derived growth factor (PDGF)-induced tyrosine phosphorylation of the low density lipoprotein receptor-related protein (LRP) Evidence for integrated co-receptor function between LRP and the PDGF, *Journal of Biological Chemistry 277*, 15499-15506.

[116] Kovacina, K. S., Park, G. Y., Bae, S. S., Guzzetta, A. W., Schaefer, E., Birnbaum, M. J., and Roth, R. A. (2003) Identification of a proline-rich Akt substrate as a 14-3-3 binding partner, *Journal of Biological Chemistry 278*, 10189-10194.

[117] Cantley, L. C. (2002) The phosphoinositide 3-kinase pathway, *Science 296*, 1655-1657.

[118] Wang, H., Zhang, Q., Wen, Q., Zheng, Y., Lazarovici, P., Jiang, H., Lin, J., and Zheng, W. (2012) Proline-rich Akt substrate of 40kDa (PRAS40): a novel downstream target of PI3k/Akt signaling pathway, *Cellular signalling 24*, 17-24.

ASBMB MOLECULAR & CELLULAR PROTEOMICS MCP

## Figure Legends

**Figure 1: Galectin-3 revealed more significant interacting binding partners than Galectin-1.** A: Numbers of protein identifications in all Gal-1 (red) and Gal-3 (blue) pull-down experiments (left Venn diagram); numbers of protein identifications of all significantly enriched ($p<0.05$) proteins with an enrichment factor over or equal 2 in the galectin ß-lactose eluates compared to negative control ($FC\geq2$) (central Venn diagram) and of all significantly enriched proteins ($p<0.05$, $FC\geq2$ ), that could be detected in 2 or more independent pull-down experiments (right Venn diagram). Numbers of overlapping protein identifications are also represented (grey). B+C: Volcano plot representation of one exemplary Galectin-1 (A) and one exemplary Galectin -3 (B) pull-down experiment (with 3 replicates each). The log2 transformed ratios between normalized abundances of all proteins identified in lactose eluates of galectin pull-down compared to unspecific control (Protein-G pull-down) is plotted against the respective negative log10 transformed p-values of the t-test. P-values of $p<0.05$ and additional regulation of ≥ two fold were regarded as significant (red dots). Infinite fold changes were set to the highest measured ratio plus 1 (dots on the right site of the plot), fold changes with a value of 0 were equalized with the lowest measured ratio (dots on the left site of the plot).

**Figure 2: Galectin interactors play a role in multiple binding processes and are mainly localized in membranes.** 15 proteins could be identified as potential Gal-1 interactors, 131 proteins as potential Gal-3 interactors. A: Comparison of the 15 Galectin-1 interactors (inner chart) and the 131 Galectin-3 interactors (outer chart), based on the gene ontology (GO) annotation “cellular component” in FunRich[64]. B+C: Network of Galectin-1 (B) and Galectin-3 (C) interactors, clustered by the GO term “molecular function” in the cytoscape app ClueGo-CluePedia[65]. The size of the nodes represents the statistical significance of the enrichment of the terms. The group heading term is the most significant within a group (default). The color

ASBMB MOLECULAR & CELLULAR PROTEOMICS MCP

code reflects the functional groups. The edges show the connection of distinct genes to specific molecular functions. Identified Gal-1 interactors that were not connected to other proteins in the Gal-1 network: LGALS3BP, LAMP2, GBA, LANCL1, MLEC, SSBP1. Identified Gal-3 interactors that were not connected to other proteins in the Gal-3 network: PLXDC2, TGM2, BSG, SRM, RAB5C, QSOX1, PTGFRN, ACP2, MCAM, LOX, LGALS3BP, SEZ6L2, MXRA5, NCSTN, AFP, DCBLD2, ARL6IP5, TMEM179B.

**Figure 3: Exogenous Galectin-1 and Galectin-3 induce cross-linking of LRP1 and ITGB1 on the cell surface of human mesenchymal RPE cells.** Immunocytochemical staining of human RPE cells, pretreated before fixation with or without biotinylated Gal-1 or Gal-3 for 30 min. Galectin-binding was visualized by Streptavidin-Alexa488 (green), LRP1 by Alexa647 (magenta) and ITGB1 by Alexa568 (red). Gal-1 and Gal-3 (B and C), LRP1 (E and F) and ITGB1 (H and I) stainings show a pronounced punctuate staining pattern. Double staining of RPE cells with Gal-1/Gal-3 and LRP1 as well as with Gal-1/Gal-3 and ITGB1 indicated a clear overlay of both staining patterns, visible by white (K and L) and yellow (N and O) spots. For visualization of the clustering of galectin, LRP1 and ITGB1, LRP1 staining was changed in silico to blue and the overlay is seen in white (Q and R). Whereas exogenous addition of galectin led to clear co-localization of LRP1 and ITGB1 on human RPE cells, no crosslinking could be seen without exogenous galectin (J, M and P). Representative images from 4 independent experiments are shown. Scale bar: 10µm.

**Figure 4: Complex-type N-glycosylation of Galectin-interactors is required for Galectin-binding**. Gal-1 and Gal-3 pull-down experiments with lysates of human RPE cells, treated or untreated with 10µM Kifunensine. The eluates were analyzed by Western Blot with antibodies against PDGFRB and LRP1. 10µg of the whole cell extracts of the respective cell types were

ASBMB MOLECULAR & CELLULAR PROTEOMICS MCP

used as an input control for the pull-down experiments and probed for GAPDH as loading control. Representative blots from three independent experiments are shown.

**Figure 5: Complex-type N-glycosylation of Galectin-interactors is necessary for Galectin induced cross-linking of LRP1 and ITGB1 on the cell surface of mesenchymal RPE cells.** Immunocytochemical staining of human RPE cells, pretreated with 10µM Kifunensine. Before fixation cells were pretreated with biotinylated Gal-1 or Gal-3 for 30 min. Galectin-binding was visualized with Streptavidin-Alexa488 (green) (A-D), LRP1 by Alexa647 (magenta) (A1-D1) and ITGB1 by Alexa568 (red) (A2-D2). Overlay of LRP1 and galectin staining patterns is visible in white (A4-D4), overlay of ITGB1 and galectin staining patterns in yellow (A3-D3). For visualization of the clustering of galectin, LRP1 and ITGB1, LRP1 staining was changed in silico to blue and the overlay is seen in white (A5-D5). Whereas addition of exogenous galectin led to clear co-localization of LRP1 and ITGB1 on human RPE cells not treated with Kifunensine (B-B5 and D-D5), no crosslinking could be observed in RPE cells treated with Kifunensine (A-A5 and C-C5). Representative images from 2 independent experiments are shown. Scale bar: 10µm.

**Figure 6: Enhanced phosphorylation of ERK-1/2 and AKT-1/2/3 by binding of Gal-1 and Gal-3.** Analysis of phosphorylation levels induced by Gal-1 or Gal-3 treatment by Western Blot. A: 300µg of ARPE19 cell extracts untreated or treated with Gal-1 or Gal-3 for 15 minutes were incubated with a nitrocellulose membrane of the Human Phospho-Kinase Array. Profiling of phosphorylation levels revealed significant induction of ERK1/2, GSK-3α/β, Pras-40 and Akt-1/2/3 phosphorylation after treatment with Gal-1 or Gal-3. The amount of phosphorylated protein bound at the respective capture spot was visualized by signal development with chemiluminescent detection reagents and mean pixel density was determined in duplicates. P-values lower than 0.05 were considered as significant (*), p-values lower than 0.01 as highly

ASBMB
MOLECULAR & CELLULAR PROTEOMICS
MCP

significant (**). B: 15µg of whole cell extracts of ARPE19 cells untreated or treated with Gal-1 or Gal-3 for 1, 15 or 30 minutes were separated by SDS-PAGE (10% gels) and blotted onto PVDF membranes. Blots were incubated with antibodies against phospho-ERK p44/p42 and GAPDH. Representative blots from three independent experiments are shown.

ASBMB MOLECULAR & CELLULAR PROTEOMICS MCP

## Tables

**Table 1: List of RPE cell proteins with high affinity to Galectin-1.**

| 1st Accession Number | Gene name | Ratio Gal1/neg. control | P-value | TMD | SP | Protein name |
|---|---|---|---|---|---|---|
| ENSP00000333298 | LAMP1 | 1065.8 | 0.006 | 1 | Y | lysosomal-associated membrane protein 1 |
| ENSP00000307513 | MRC2 | 136.4 | 0.049 | 1 | 0 | mannose receptor, C type 2 |
| ENSP00000007722 | ITGA3 | 104.6 | 0.021 | 1 | Y | integrin, alpha 3 |
| ENSP00000261023 | ITGAV | 59.2 | 0.016 | 1 | Y | integrin, alpha V |
| ENSP00000303351 | ITGB1 | 53.9 | 0.014 | 1 | Y | integrin, beta 1 |
| ENSP00000233714 | LANCL1 | 52.2 | 0.001 | 0 | 0 | LanC l antibiotic synthetase component C-like 1 (bacterial) |
| ENSP00000314508 | GBA | 34.8 | 0.000 | 0 | Y | glucosidase, beta, acid |
| ENSP00000331544 | FBLN1 | 34.1 | 0.018 | 0 | Y | fibulin 1 |
| ENSP00000243077 | LRP1 | 31.1 | 0.019 | 1 | Y | low density lipoprotein receptor-related protein 1 |
| ENSP00000258341 | LAMC1 | 21.3 | 0.002 | 0 | Y | laminin, gamma 1 (formerly LAMB2) |
| ENSP00000262776 | LGALS3BP | 19.0 | 0.043 | 0 | Y | lectin, galactoside-binding, soluble, 3 binding protein |
| ENSP00000228506 | MLEC | 18.1 | 0.037 | 1 | Y | malectin |
| ENSP00000265304 | SSBP1 | 6.1 | 0.045 | 0 | 0 | single-stranded DNA binding protein 1, mitochondrial |
| ENSP00000200639 | LAMP2 | 5.9 | 0.001 | 1 | Y | lysosomal-associated membrane protein 2 |
| ENSP00000258733 | GPNMB | 5.3 | 0.049 | 1 | Y | glycoprotein (transmembrane) nmb |

15 identified Gal-1 interactors in order of their enrichment factors in the ß-lactose eluates of galectin pull-downs compared to unspecific controls. For calculation the mean of all technical replicates within one experiment was used. Significance was determined by Student's t-test. Proteins with p-values of $p<0.05$, enrichment of ≥ two-fold in galectin pull-down eluates (FC ≥ 2) and additional identification in two or more independent pull-down experiments (n ≥ 2), were regarded as significant. The ratios represent the maximum fold changes of all experiments and the corresponding p-values. TMD: transmembrane domain. SP: signal peptide. FC: fold change.

**Table 2: List of RPE cell proteins with high affinity to Galectin-3.**

| 1st Accession Number | gene name | Ratio Gal3/neg. control | P-value | TMD | SP | Protein name |
|---|---|---|---|---|---|---|
| ENSP00000273784 | AHSG | infinity | 0.016 | 0 | Y | alpha-2-HS-glycoprotein |
| ENSP00000222374 | CADM4 | infinity | 0.047 | 1 | Y | cell adhesion molecule 4 |
| ENSP00000312435 | DAG1 | infinity | 0.004 | 1 | Y | dystroglycan 1 (dystrophin-associated glycoprotein 1) |
| ENSP00000321573 | DCBLD2 | infinity | 0.007 | 3 | Y | discoidin, CUB and LCCL domain containing 2 |
| ENSP00000334145 | F3 | infinity | 0.003 | 1 | 0 | coagulation factor III (thromboplastin, tissue factor) |
| ENSP00000314508 | GBA | infinity | 0.014 | 0 | Y | glucosidase, beta, acid |
| ENSP00000282588 | ITGA1 | infinity | 0.002 | 1 | Y | integrin, alpha 1 |
| ENSP00000264106 | ITGA6 | infinity | 0.015 | 1 | Y | integrin, alpha 6 |
| ENSP00000266041 | ITIH4 | infinity | 0.014 | 0 | Y | inter-alpha-trypsin inhibitor heavy chain family, member 4 |
| ENSP00000258341 | LAMC1 | infinity | 0.016 | 0 | Y | laminin, gamma 1 (formerly LAMB2) |
| ENSP00000231004 | LOX | infinity | 0.046 | 0 | Y | lysyl oxidase |
| ENSP00000374135 | LRP1B | infinity | 0.029 | 1 | Y | low density lipoprotein receptor-related protein 1B |
| ENSP00000199940 | MAP2 | infinity | 0.035 | 0 | 0 | microtubule-associated protein 2 |
| ENSP00000217939 | MXRA5 | infinity | 0.012 | 0 | Y | matrix-remodelling associated 5 |
| ENSP00000294785 | NCSTN | infinity | 0.009 | 1 | Y | nicastrin |
| ENSP00000324270 | OXTR | infinity | 0.041 | 7 | 0 | oxytocin receptor |
| ENSP00000319782 | PODXL | infinity | 0.020 | 1 | Y | podocalyxin-like |
| ENSP00000356572 | QSOX1 | infinity | 0.007 | 0 | Y | quiescin Q6 sulfhydryl oxidase 1 |
| ENSP00000266771 | SLC15A4 | infinity | 0.014 | 13 | 0 | solute carrier family 15 (oligopeptide transporter), member 4 |
| ENSP00000444408 | SLC1A5 | infinity | 0.017 | 9 | 0 | solute carrier family 1 (neutral amino acid transporter), member 5 |
| ENSP00000004531 | SLC7A2 | infinity | 0.042 | 14 | 0 | solute carrier family 7 (cationic amino acid transporter, y+ system), member 2 |
| ENSP00000335300 | TPCN1 | infinity | 0.002 | 12 | 0 | two pore segment channel 1 |
| ENSP00000351190 | ITIH2 | 527961.6 | 0.006 | 0 | Y | inter-alpha-trypsin inhibitor heavy chain 2 |
| ENSP00000418725 | ITGB1 | 20223.9 | 0.011 | 0 | Y | integrin, beta 1 (fibronectin receptor, beta polypeptide, antigen CD29 includes MDF2, MSK12) |
| ENSP00000269141 | CDH2 | 4103.6 | 0.003 | 1 | Y | cadherin 2, type 1, N-cadherin (neuronal) |
| ENSP00000257857 | CD63 | 3186.1 | 0.032 | 4 | 0 | CD63 molecule |
| ENSP00000329797 | CADM1 | 2304.6 | 0.003 | 1 | Y | cell adhesion molecule 1 |
| ENSP00000333298 | LAMP1 | 1591.0 | 0.003 | 1 | Y | lysosomal-associated membrane protein 1 |
| ENSP00000231368 | LNPEP | 1439.2 | 0.031 | 1 | 0 | leucyl/cystinyl aminopeptidase |
| ENSP00000257879 | ITGA7 | 1433.6 | 0.000 | 1 | 0 | integrin, alpha 7 |
| ENSP00000256689 | SLC38A2 | 910.1 | 0.015 | 11 | 0 | solute carrier family 38, member 2 |
| ENSP00000268613 | CDH13 | 900.6 | 0.008 | 0 | 0 | cadherin 13 |
| ENSP00000368752 | PRNP | 737.3 | 0.024 | 2 | Y | prion protein |
| ENSP00000263398 | CD44 | 581.2 | 0.017 | 1 | Y | CD44 molecule (Indian blood group) |
| ENSP00000382340 | ABCC1 | 521.0 | 0.002 | 10 | 0 | ATP-binding cassette, sub-family C (CFTR/MRP), member 1 |
| ENSP00000293379 | ITGA5 | 477.1 | 0.002 | 1 | Y | integrin, alpha 5 (fibronectin receptor, alpha polypeptide) |



ASBMB MOLECULAR & CELLULAR PROTEOMICS MCP

| | | | | | | |
|---|---|---|---|---|---|---|
| ENSP00000230418 | PTK7 | 231.3 | 0.005 | 1 | Y | protein tyrosine kinase 7 |
| ENSP00000261978 | LTBP2 | 219.4 | 0.002 | 0 | Y | latent transforming growth factor beta binding protein 2 |
| ENSP00000280527 | CRIM1 | 218.6 | 0.003 | 1 | Y | cysteine rich transmembrane BMP regulator 1 (chordin-like) |
| ENSP00000308727 | SUSD5 | 218.1 | 0.001 | 1 | Y | sushi domain containing 5 |
| ENSP00000336888 | SLC44A2 | 208.8 | 0.006 | 10 | 0 | solute carrier family 44 (choline transporter), member 2 |
| ENSP00000258733 | GPNMB | 202.7 | 0.007 | 1 | Y | glycoprotein (transmembrane) nmb |
| ENSP00000256997 | ACP2 | 198.2 | 0.026 | 1 | Y | acid phosphatase 2, lysosomal |
| ENSP00000357190 | PTPRK | 197.0 | 0.040 | 1 | Y | protein tyrosine phosphatase, receptor type, K |
| ENSP00000356787 | ATP1B1 | 188.5 | 0.044 | 1 | 0 | ATPase, Na+/K+ transporting, beta 1 polypeptide |
| ENSP00000310206 | SEZ6L2 | 184.0 | 0.041 | 1 | Y | seizure related 6 homolog (mouse)-like 2 |
| ENSP00000306864 | VASN | 180.9 | 0.024 | 1 | Y | vasorin |
| ENSP00000348307 | SIRPA | 146.7 | 0.044 | 1 | Y | signal-regulatory protein alpha |
| ENSP00000421922 | LRPAP1 | 141.9 | 0.001 | 0 | Y | low density lipoprotein receptor-related protein associated protein 1 |
| ENSP00000320084 | CD276 | 121.5 | 0.010 | 1 | Y | CD276 molecule |
| ENSP00000305988 | ALCAM | 121.5 | 0.007 | 1 | Y | activated leukocyte cell adhesion molecule |
| ENSG00000125730 | C3 | 119.1 | 0.042 | 0 | Y | complement component 3 |
| ENSP00000290401 | NPTN | 115.6 | 0.002 | 1 | Y | neuroplastin |
| ENSP00000378392 | PSAP | 111.3 | 0.002 | 0 | Y | prosaposin |
| ENSP00000264036 | MCAM | 109.0 | 0.022 | 1 | Y | melanoma cell adhesion molecule |
| ENSP00000311502 | HEG1 | 101.8 | 0.003 | 0 | 0 | heart development protein with EGF-like domains 1 |
| ENSP00000331544 | FBLN1 | 100.3 | 0.015 | 0 | Y | fibulin 1 |
| ENSP00000311402 | SLC4A2 | 96.9 | 0.046 | 13 | 0 | solute carrier family 4 (anion exchanger), member 2 |
| ENSP00000228506 | MLEC | 96.6 | 0.000 | 1 | Y | malectin |
| ENSP00000053867 | GRN | 85.3 | 0.013 | 0 | Y | granulin |
| ENSP00000296181 | ITGB5 | 84.8 | 0.001 | 1 | Y | integrin, beta 5 |
| ENSP00000265077 | VCAN | 83.4 | 0.003 | 0 | Y | versican |
| ENSP00000295633 | FSTL1 | 77.8 | 0.008 | 0 | Y | follistatin-like 1 |
| ENSP00000413922 | ITIH3 | 76.7 | 0.024 | 0 | Y | inter-alpha-trypsin inhibitor heavy chain 3 |
| ENSP00000352288 | PLXNB2 | 75.0 | 0.005 | 1 | Y | plexin B2 |
| ENSP00000318557 | SLC12A4 | 74.5 | 0.013 | 14 | 0 | solute carrier family 12 (potassium/chloride transporter), member 4 |
| ENSP00000324101 | CD151 | 72.1 | 0.028 | 4 | 0 | CD151 molecule (Raph blood group) |
| ENSP00000266718 | LUM | 65.3 | 0.001 | 0 | Y | lumican |
| ENSP00000273258 | ARL6IP5 | 60.8 | 0.049 | 4 | 0 | ADP-ribosylation-like factor 6 interacting protein 5 |
| ENSP00000269228 | NPC1 | 60.7 | 0.009 | 13 | Y | Niemann-Pick disease, type C1 |
| ENSP00000347596 | EFEMP1 | 57.1 | 0.004 | 0 | Y | EGF containing fibulin-like extracellular matrix protein 1 |
| ENSP00000333697 | TMEM179B | 52.2 | 0.007 | 3 | Y | transmembrane protein 179B |
| ENSP00000312506 | CSPG4 | 44.1 | 0.003 | 1 | Y | chondroitin sulfate proteoglycan 4 |
| ENSP00000188790 | FAP | 43.6 | 0.022 | 0 | Y | fibroblast activation protein, alpha |
| ENSP00000323534 | FN1 | 43.3 | 0.002 | 0 | Y | fibronectin 1 |



ASBMB MOLECULAR & CELLULAR PROTEOMICS MCP

| | | | | | | |
|---|---|---|---|---|---|---|
| ENSP00000262776 | LGALS3BP | 41.9 | 0.004 | 0 | Y | lectin, galactoside-binding, soluble, 3 binding protein |
| ENSP00000243077 | LRP1 | 41.5 | 0.001 | 1 | Y | low density lipoprotein receptor-related protein 1 |
| ENSP00000315130 | CLU | 39.7 | 0.002 | 0 | Y | clusterin |
| ENSP00000206423 | CCDC80 | 38.8 | 0.001 | 0 | Y | coiled-coil domain containing 80 |
| ENSP00000318646 | RPS15A | 37.8 | 0.003 | 0 | 0 | ribosomal protein S15a |
| ENSP00000200639 | LAMP2 | 37.6 | 0.004 | 1 | Y | lysosomal-associated membrane protein 2 |
| ENSP00000307513 | MRC2 | 37.5 | 0.002 | 1 | 0 | mannose receptor, C type 2 |
| ENSP00000261023 | ITGAV | 32.1 | 0.015 | 1 | Y | integrin, alpha V |
| ENSP00000341730 | RPL10 | 31.6 | 0.003 | 0 | 0 | ribosomal protein L10 |
| ENSP00000371626 | TRA2B | 31.4 | 0.006 | 0 | 0 | transformer 2 beta homolog (Drosophila) |
| ENSP00000323929 | A2M | 30.9 | 0.002 | 0 | Y | alpha-2-macroglobulin |
| ENSP00000333769 | BSG | 26.8 | 0.000 | 1 | Y | basigin (Ok blood group) |
| ENSP00000007722 | ITGA3 | 26.7 | 0.001 | 1 | Y | integrin, alpha 3 (antigen CD49C, alpha 3 subunit of VLA-3 receptor) |
| ENSP00000349437 | IGF2R | 26.5 | 0.003 | 1 | Y | insulin-like growth factor 2 receptor |
| ENSP00000084795 | RPL18 | 25.6 | 0.000 | 0 | 0 | ribosomal protein L18 |
| ENSP00000222399 | LAMB1 | 24.9 | 0.000 | 0 | Y | laminin, beta 1 |
| ENSP00000226359 | AFP | 22.1 | 0.013 | 0 | Y | alpha-fetoprotein |
| ENSP00000252804 | PXDN | 21.3 | 0.006 | 0 | Y | peroxidasin |
| ENSP00000275730 | SLC12A9 | 20.8 | 0.003 | 13 | 0 | solute carrier family 12, member 9 |
| ENSP00000359602 | LMBRD1 | 19.6 | 0.013 | 7 | 0 | LMBR1 domain containing 1 |
| ENSP00000366460 | PLXDC2 | 19.2 | 0.007 | 1 | Y | plexin domain containing 2 |
| ENSP00000286371 | ATP1B3 | 18.8 | 0.035 | 1 | 0 | ATPase, Na+/K+ transporting, beta 3 polypeptide |
| ENSP00000264896 | SCARB2 | 15.7 | 0.026 | 1 | Y | scavenger receptor class B, member 2 |
| ENSP00000340815 | SLC3A2 | 15.6 | 0.012 | 1 | 0 | solute carrier family 3 (amino acid transporter heavy chain), member 2 |
| ENSP00000327290 | ITGA11 | 15.2 | 0.016 | 1 | Y | integrin, alpha 11 |
| ENSP00000260356 | THBS1 | 15.2 | 0.002 | 0 | Y | thrombospondin 1 |
| ENSP00000341861 | SERPING1 | 13.7 | 0.041 | 0 | Y | serpin peptidase inhibitor, clade G (C1 inhibitor), member 1 |
| ENSP00000376899 | PTGFRN | 13.3 | 0.016 | 1 | Y | prostaglandin F2 receptor inhibitor |
| ENSP00000377047 | PTPRZ1 | 13.1 | 0.048 | 1 | Y | protein tyrosine phosphatase, receptor-type, Z polypeptide 1 |
| ENSP00000296585 | ITGA2 | 12.1 | 0.003 | 1 | Y | integrin, alpha 2 (CD49B, alpha 2 subunit of VLA-2 receptor) |
| ENSP00000261799 | PDGFRB | 11.7 | 0.012 | 1 | Y | platelet-derived growth factor receptor, beta polypeptide |
| ENSP00000355330 | TGM2 | 11.4 | 0.001 | 0 | 0 | transglutaminase 2 |
| ENSP00000222247 | RPL18A | 10.2 | 0.001 | 0 | 0 | ribosomal protein L18a |
| ENSP00000344456 | CTNNB1 | 9.1 | 0.000 | 0 | 0 | catenin (cadherin-associated protein), beta 1, 88kDa |
| ENSP00000272317 | RPS27A | 8.8 | 0.006 | 0 | 0 | ribosomal protein S27a |
| ENSP00000264832 | ICAM1 | 6.7 | 0.000 | 1 | Y | intercellular adhesion molecule 1 |
| ENSP00000296674 | RPS23 | 6.4 | 0.016 | 0 | 0 | ribosomal protein S23 |
| ENSP00000346015 | RPL27A | 5.9 | 0.000 | 0 | 0 | ribosomal protein L27a |
| ENSP00000369743 | RPS6 | 4.8 | 0.001 | 0 | 0 | ribosomal protein S6 |



ASBMB MOLECULAR & CELLULAR PROTEOMICS MCP

| | | | | | | |
|---|---|---|---|---|---|---|
| ENSP00000253788 | RPL27 | 4.8 | 0.003 | 0 | 0 | ribosomal protein L27 |
| ENSP00000416293 | SLC2A1 | 4.5 | 0.010 | 12 | 0 | solute carrier family 2 (facilitated glucose transporter), member 1 |
| ENSP00000311430 | RPL4 | 4.3 | 0.027 | 0 | 0 | ribosomal protein L4 |
| ENSP00000277865 | GLUD1 | 4.2 | 0.036 | 0 | Y | glutamate dehydrogenase 1 |
| ENSP00000345689 | RAB5C | 4.2 | 0.026 | 0 | 0 | RAB5C, member RAS oncogene family |
| ENSP00000363018 | RPL10A | 3.8 | 0.006 | 0 | 0 | ribosomal protein L10a |
| ENSP00000348849 | RPS26 | 3.8 | 0.024 | 0 | 0 | ribosomal protein S26 |
| ENSP00000225698 | C1QBP | 3.4 | 0.027 | 0 | 0 | complement component 1, q subcomponent binding protein |
| ENSP00000346022 | RPL9 | 3.4 | 0.011 | 0 | 0 | ribosomal protein L9 |
| ENSP00000295598 | ATP1A1 | 3.3 | 0.003 | 8 | 0 | ATPase, Na+/K+ transporting, alpha 1 polypeptide |
| ENSP00000379888 | RPS8 | 3.2 | 0.026 | 0 | 0 | ribosomal protein S8 |
| ENSP00000305920 | GLB1 | 3.1 | 0.047 | 0 | Y | galactosidase, beta 1 |
| ENSP00000325136 | HADHB | 3.1 | 0.030 | 0 | Y | hydroxyacyl-CoA dehydrogenase/3-ketoacyl-CoA thiolase/enoyl-CoA hydratase (trifunctional protein), beta subunit |
| ENSP00000346027 | RPL21 | 3.1 | 0.036 | 0 | 0 | ribosomal protein L21 |
| ENSP00000366156 | SRM | 3.1 | 0.038 | 0 | 0 | spermidine synthase |
| ENSP00000251453 | RPS16 | 2.5 | 0.040 | 0 | 0 | ribosomal protein S16 |
| ENSP00000342070 | CTSB | 2.5 | 0.004 | 0 | Y | cathepsin B |

131 identified Gal-3 interactors in order of their enrichment factors in the lactose eluates of galectin pull-downs compared to unspecific controls. For calculation the mean of all technical replicates within one experiment was used. Significance was determined by Student's t-test. Proteins with p-values of $p<0.05$, enrichment of ≥ two-fold in galectin pull-down eluates (FC ≥ 2) and additional identification in two or more independent pull-down experiments (n ≥ 2), were regarded as significant. The ratios represent the maximum fold changes of all experiments and the corresponding p-values. TMD: transmembrane domain. SP: signal peptide. FC: fold change.



ASBMB MOLECULAR & CELLULAR PROTEOMICS MCP

ASBMB
MOLECULAR & CELLULAR PROTEOMICS
MCP

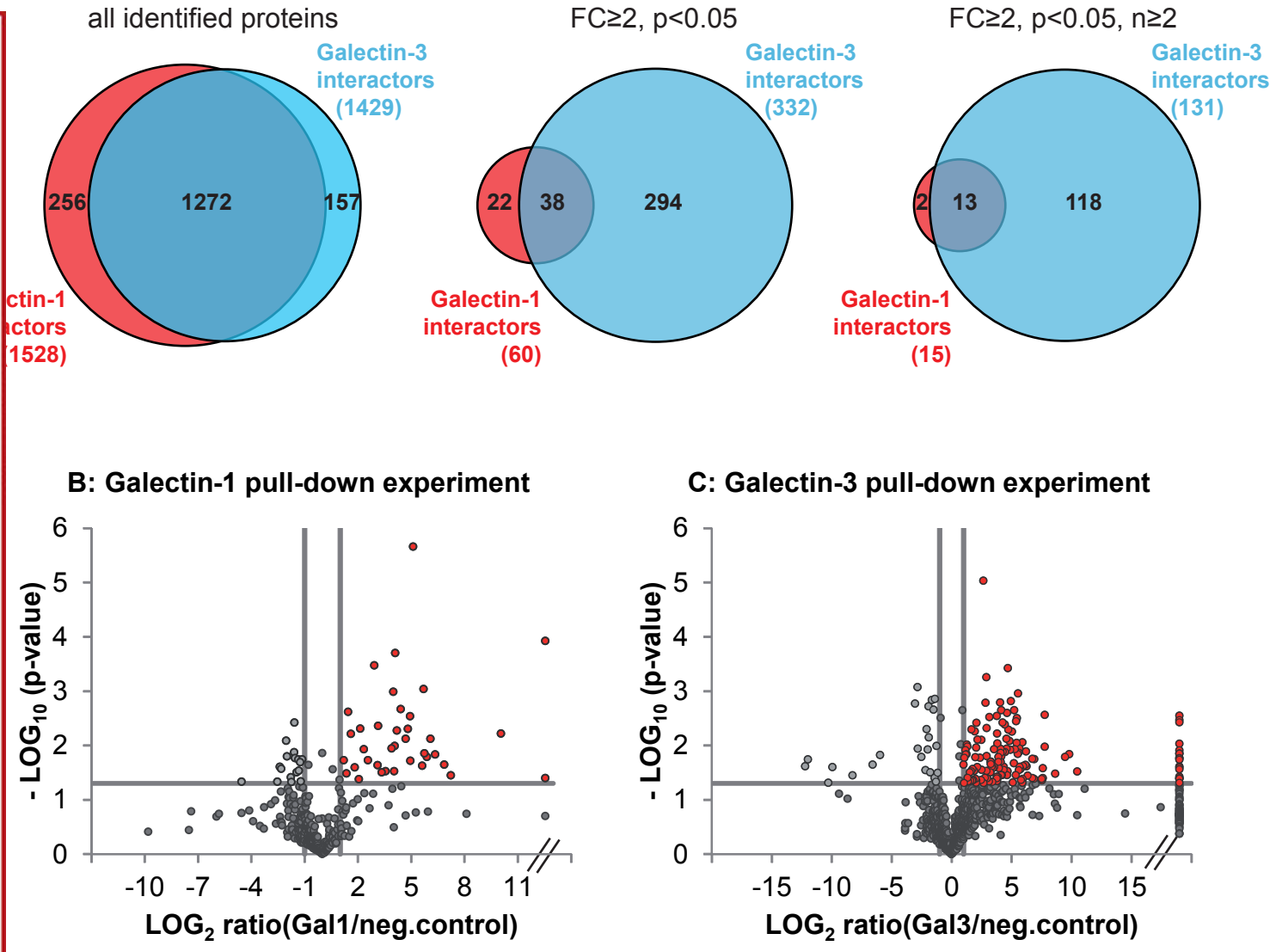


Figure 1

ASBMB
MOLECULAR & CELLULAR PROTEOMICS
MCP

## A: Cellular component comparison

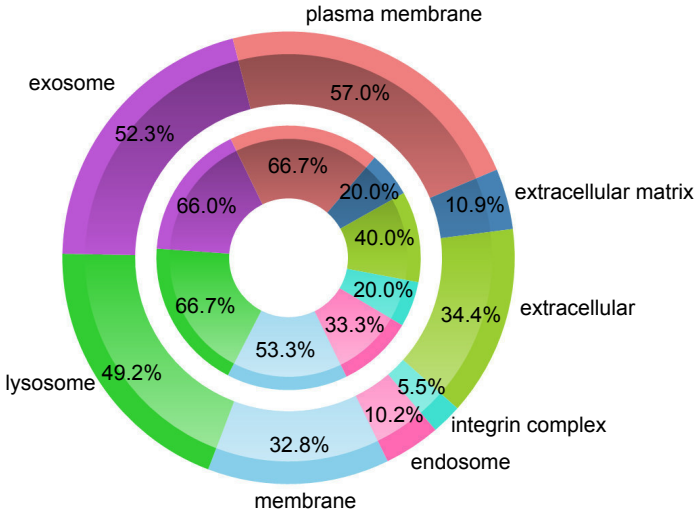


Galectin-3 interactors on outer chart, Galectin-1 interactors on inner chart

## B: Galectin-1 interactors

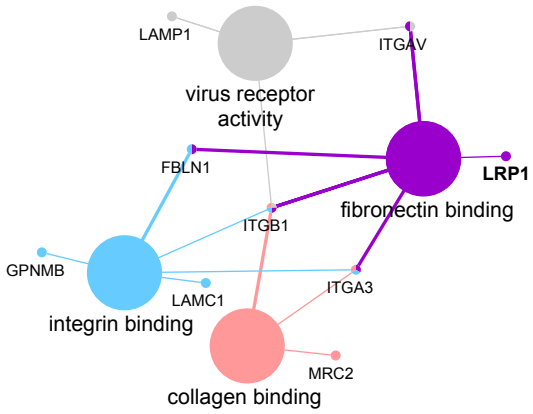


## Galectin-3 interactors

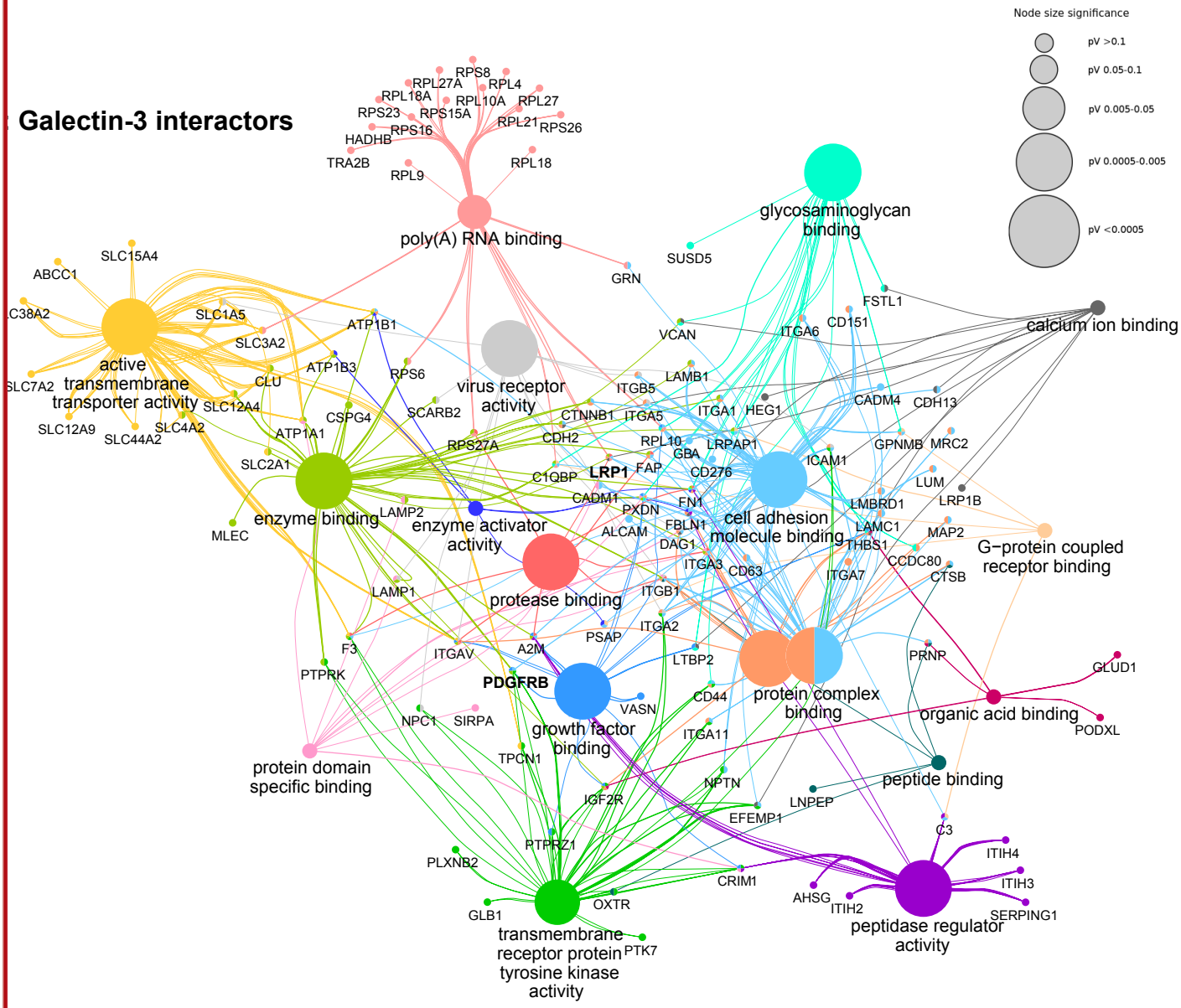


figure 2

ASBMB
MOLECULAR & CELLULAR PROTEOMICS
MCP

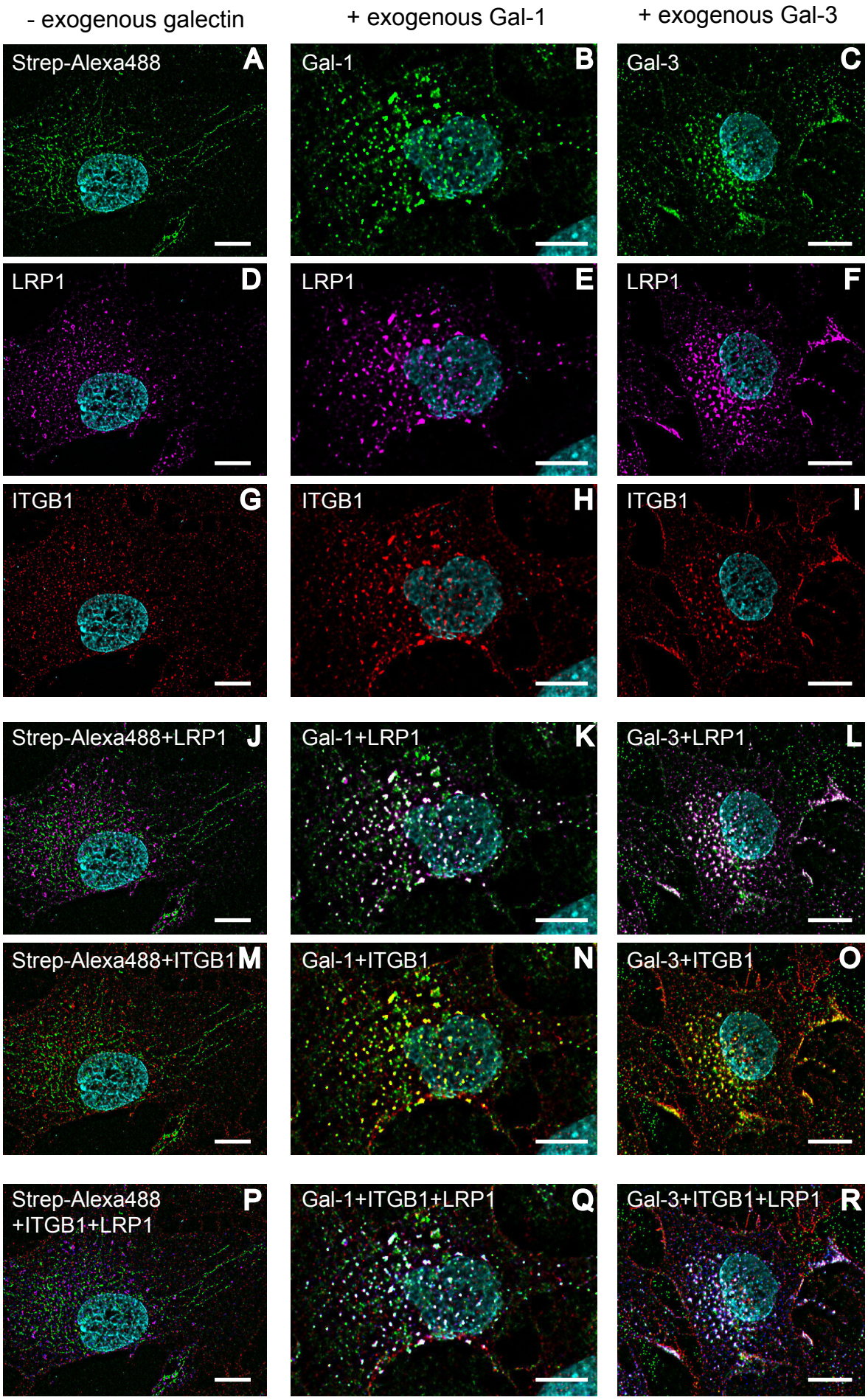


figure 3

ASBMB
MOLECULAR & CELLULAR PROTEOMICS
MCP




figure 4

ASBMB
MOLECULAR & CELLULAR PROTEOMICS
MCP

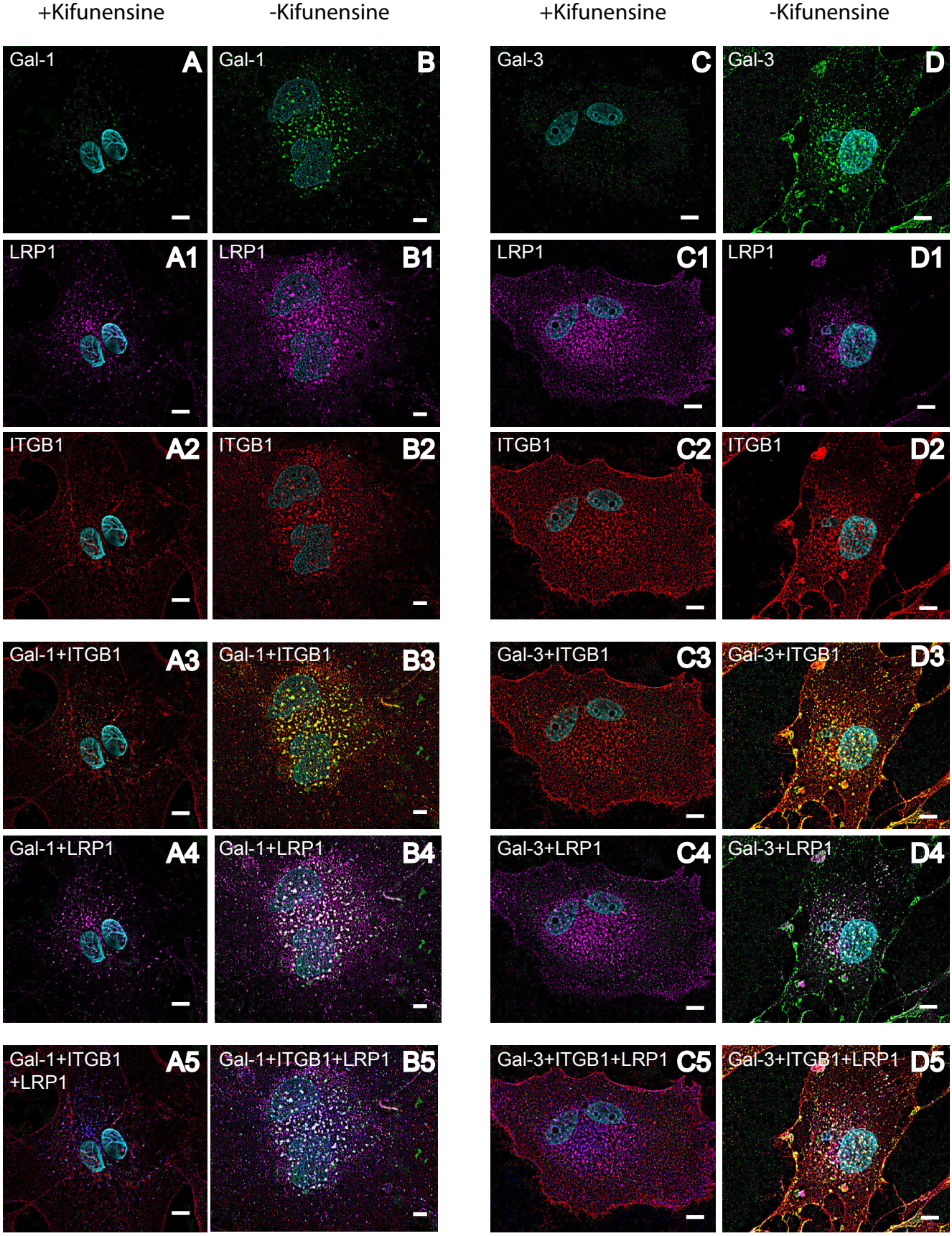


figure 5

A

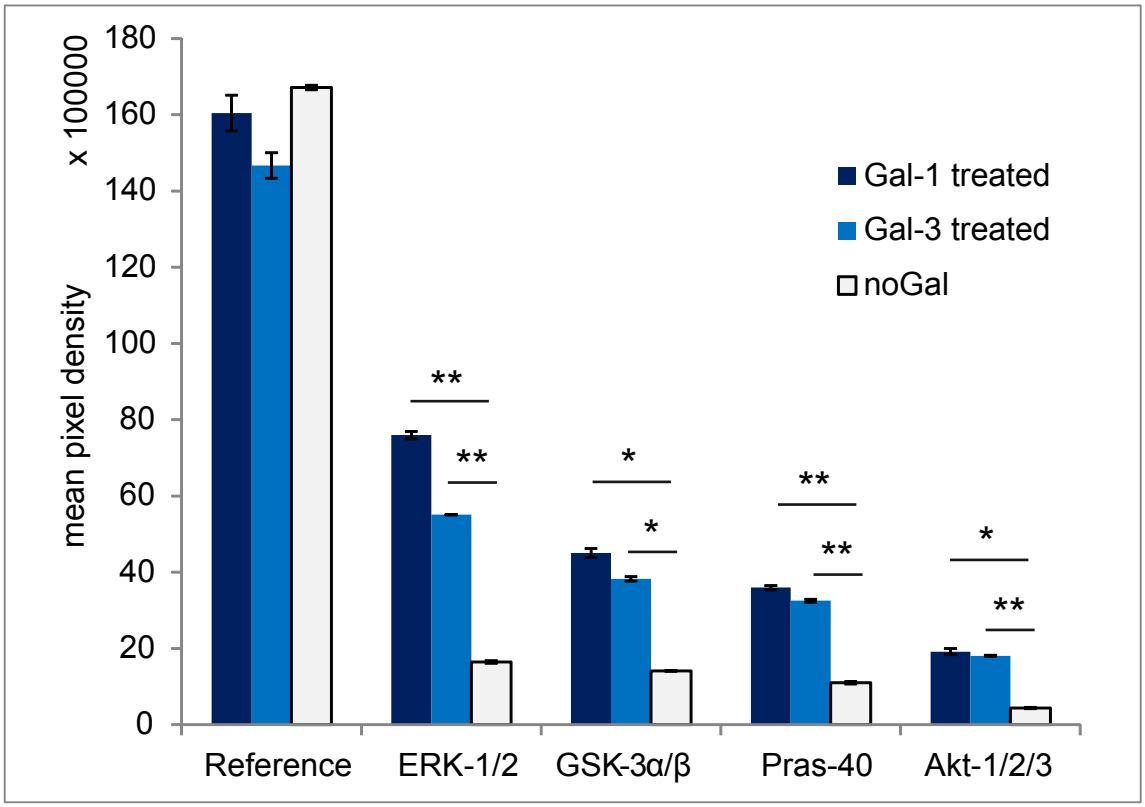


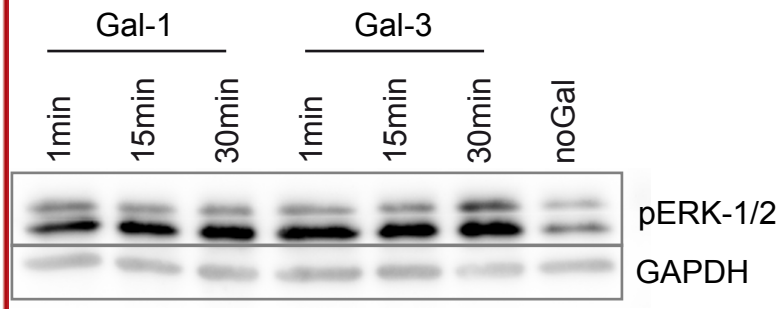


figure 6

ASBMB
MOLECULAR & CELLULAR PROTEOMICS
MCP